An advanced sequence clustering and designation workflow reveals the enzootic maintenance of a dominant West Nile virus subclade in Germany

Pauline Dianne Santos[1,†], Anne Günther[1,†], Markus Keller[2], Timo Homeier-Bachmann[3], Martin H. Groschup[2,4], Martin Beer[1], Dirk Höper[1,†], Ute Ziegler[2,4, †,*]

[1] Friedrich-Loeffler-Institut, Federal Research Institute for Animal Health, Institute of Diagnostic Virology, 17493 Greifswald-Insel Riems, Germany; pauline.santos@pei.de, anne.guenther@fli.de, dirk.hoeper@fli.de, martin.beer@fli.de

[2] Friedrich-Loeffler-Institut, Federal Research Institute for Animal Health, Institute of Novel and Emerging Infectious Diseases, 17493 Greifswald-Insel Riems, Germany; markus.keller@fli.de, martin.groschup@fli.de, ute.ziegler@fli.de

[3] Friedrich-Loeffler-Institut, Federal Research Institute for Animal Health, Institute of Epidemiology, 17493 Greifswald-Insel Riems, Germany; timo.homeier@fli.de

[4] German Centre for Infection Research, partner site Hamburg-Lübeck-Borstel-Riems, 17493 Greifswald-Insel Riems, Germany

* Correspondence: ute.ziegler@fli.de; Tel.: +49-38351-71519

† These authors contributed equally to this work.

Abstract

West Nile virus (WNV) is the most widespread arthropod-borne (arbo) virus and the primary cause of arboviral encephalitis globally. Members of WNV species genetically diverged and are classified into different hierarchical groups below species rank. However, the demarcation criteria for allocating WNV sequences into these groups remain individual, inconsistent, and the use of names for different levels of the hierarchical levels is unstructured. In order to have an objective and comprehensible grouping of WNV sequences, we developed an advanced grouping workflow using the “affinity propagation clustering”-algorithm and newly included the “agglomerative hierarchical clustering”-algorithm for the allocation of WNV sequences into different groups below species rank. In addition, we propose to use a fixed set of terms for the hierarchical naming of WNV below species level and a clear decimal numbering system to label the determined groups. For validation, we applied the refined workflow to WNV sequences that have been previously grouped into various lineages, clades, and clusters in other studies. Although our workflow regrouped some WNV sequences, overall, it generally corresponds with previous groupings. We employed our novel approach to the sequences from the WNV circulation in Germany 2020, primarily from WNV-infected birds and horses. Besides two newly defined minor (sub)clusters comprising only of three sequences each, subcluster 2.5.3.4.3c was the predominant WNV sequence group detected in Germany from 2018-20. This predominant subcluster was also associated with at least five human WNV-infections in 2019-20. In summary, our analyses imply that the genetic diversity of the WNV population in Germany is shaped by enzootic maintenance of the dominant WNV subcluster accompanied by sporadic incursions of other rare clusters and subclusters. Moreover, we show that our refined approach for sequence grouping yields meaningful results. Although we primarily aimed at a more detailed WNV classification, the presented workflow can also be applied to the objective genotyping of other virus species.

1. Introduction

Like other members of the genus *Flavivirus*, West Nile virus (WNV) has become a serious emerging zoonotic threat in Europe within the last decades (European Centre for Disease Prevention and Control n.d.; Kuno et al. 1998). The first known case of WNV-infection was reported in Uganda, Africa, in 1937 (Bardos et al. 1959; Smithburn et al. 1940). In the 1960s, the first occurrence of WNV in Europe was recognized due to neurological disorders in wild and domestic horses in France (Murgue et al. 2001). Around 30 years later, WNV caused the first severe outbreak of West Nile Fever (WNF) and West Nile Neuroinvasive Disease (WNND) in humans in Romania (Savage et al. 1999; Tsai et al. 1998). Since then, WNV has successfully established in various countries. Southern and eastern European countries were primarily affected by recurring WNV infections in humans, birds, and horses. The highest WNV activity in Europe was recorded in 2018 (Camp and Nowotny 2020; European Centre for Disease Prevention and Control 2019). Almost 90% of all locally acquired WNV human infections in Europe, with 166 fatal cases, were reported in Italy, Greece, and Romania (European Centre for Disease Prevention and Control 2019). In parallel to this large-scale epidemic in 2018, WNV-RNA positive birds and horses were confirmed for the first time in Germany (Ziegler et al. 2019). In 2019, a significant increase in WNV cases in birds and horses as well as the first five autochthonous WNV human infections in Germany were reported (Robert-Koch-Institut 2020; Ziegler et al. 2020). All prerequisites for endemic WNV circulation in Germany are fulfilled, including the proven vector competence of local mosquito populations (Holicki et al. 2020) and the detection of WNV genome-positive mosquito pools (Kampen et al. 2020; Ziegler et al. 2020).

WNV has a diverse host range and is widely distributed. Accordingly, members of this species are genetically diverse, allowing for the further subgrouping within the species. However, since the International Committee on Taxonomy of Viruses (ICTV) confines its responsibility to the designation and demarcation of viruses from realm to species ranks (ICTV 2020; Simmonds et al. 2017), neither a standard definition of criteria for subgrouping below the species rank nor defined designations for subgroups and their hierarchical arrangement exist. Therefore, designations for hierarchical ranks

(*e.g.*, clade, cluster, sub-type, genotype) are often used inconsistently and interchangeably, leading to misunderstandings and uncertainties as more and more whole genomes of WNV are generated. Due to its aforementioned genetic diversity, up to nine lineages have been proposed for the species *West Nile virus* (Fall et al. 2017; Mencattelli et al. 2022; Pachler et al. 2014). The designation "lineage" is mostly based on monophyletic clustering of partial or whole genome WNV sequences in phylogenetic analyses (Fall et al. 2017; Perez-Ramirez et al. 2017). However, the lineage classification of WNV strains remains controversial (Perez-Ramirez et al. 2017). Further subgrouping within the lineages is conducted to organize viruses into a hierarchical system comprising of various arbitrarily defined and designated groups. Especially within and between members of WNV lineages 1 and 2 the designations are used inconsistently. Groups are usually defined based on branching into monophyletic groups from a common ancestor and members of groups may share common characteristics such as unique and fixed amino acid (aa) substitutions (Anez et al. 2013; Barzon et al. 2015; Chaintoutis et al. 2019; Davis et al. 2005; Di Giallonardo et al. 2016; Hadfield et al. 2019; May et al. 2011; McMullen et al. 2013; Ziegler et al. 2020). Monophyletic groups other than lineages are typically labelled using a letter, region of origin, or abbreviation of the region of origin (Fall et al. 2017; Kolodziejek et al. 2014; McMullen et al. 2013; Ravagnan et al. 2015; Zehender et al. 2017; Ziegler et al. 2019; Ziegler et al. 2020). Noteworthy, nomenclatures based on geographic origin may be misleading. For instance, a WNV sequence from Italy branched with Eastern European WNV lineage 2 sequences detected in Romania and Russia (Bakonyi and Haussig 2020; Ravagnan et al. 2015; Sikkema et al. 2020; Ziegler et al. 2020). Moreover, Ziegler and colleagues (Ziegler et al. 2020) mentioned in the study of the 2018-19 WNV epidemic in Germany that the label "Eastern German WNV Clade (EGC)", designated to a group of WNV sequences from Germany, may not be a suitable designation because "the EGC can have developed in the wider southeastern and central European hemisphere and may have been translocated only later to Eastern Germany". Hence, labels based on geographic origin may not suit the expanding geographic or undiscovered range of a WNV sequence group.

The described situation emphasizes the need for a systematic nomenclature and objective grouping of WNV sequences into hierarchical groups below the species rank. To subdivide WNV , we further developed the objective clustering workflow established by Fischer and colleagues (Fischer et al. 2018) who utilized the affinity propagation clustering (APC) algorithm (Frey and Dueck 2007) as implemented by Bodenhofer and colleagues (Bodenhofer et al. 2011). However, Fischer and colleagues found limitations of APC especially for the definition of the best suited number of clusters and therefore ultimately the definition of groups corresponding with phylogenetic analyses. To solve these issues, we refined the method to define a suitable number of groups while also incorporating agglomerative hierarchical clustering (AHC) (Bodenhofer et al. 2011) to address grouping of sequences into multiple hierarchical levels. In addition, we suggest a decimal numbering system for the hierarchical groups designated with the proposed unified and consistent labels within the WNV species. Finally, we provide an update on the WNV situation in birds and horses in Germany 2020 by applying the improved clustering workflow and our novel generic and consistent nomenclature.

2. Material and Methods

2.1 WNV screening of birds and horses

The nationwide wild bird surveillance program in Germany was established as an instantaneous reaction to the first Usutu virus (USUV) epizootic in 2011. This monitoring program became reputable also for the early detection of other zoonotic arboviruses, such as Sindbis virus and WNV. WNV infection in birds and horses is a notifiable animal disease in Germany ifdetected by RT-qPCR (real time quantitative polymerase chain reaction) and/or the identification of WNV-specific IgM in non-vaccinated horses by ELISA (enzyme-linked immunosorbent assay; i.e. detection of a recent WNV infection).

Samples from birds or horses (e.g. complete animals, organ samples, blood samples, and/or total RNA) were sent to the national reference laboratory for WNV at the Friedrich-Loeffler-Institut (FLI), Isle of

Riems, Germany, by the regional veterinary laboratories of the German federal states, and by members of the nationwide wild bird surveillance program (for details about the members see (Ziegler et al. 2022)).

2.2 Ethical statement

Bird clinics, veterinarians, wild bird rescue centers and zoos provided bird carcasses for necropsy. In Germany, no specific permits are required to examine dead birds which have been submitted for necropsy. Horse clinics and veterinarians from the regional veterinary laboratories provided horse tissue samples collected in post-mortem examinations by pathological institutions. Residual blood material was available for one case originating from a WNV-infected bird, collected primarily for diagnostic purposes and for specific treatment and prognosis.

2.3 RNA extraction and RT-qPCR

Total RNA was extracted from tissue samples (brain, spleen, liver, spinal cord, and/or kidney) and frozen (-70 °C) coagulated blood samples (cruor). For the first RNA extraction, we applied the RNeasy Mini Kit (QIAGEN) according to the manufacturer's instructions, followed by screenings for both WNV lineage 1 and 2 genomes using an RT-qPCR assay (Eiden et al. 2010).

2.4 Whole-genome sequencing

To cover areas with and without previous WNV cases, WNV RNA positive samples from 2020 (Table 1) were selected for whole-genome sequencing (WGS) primarily based on their geographical location and C_q values. In addition, samples from captive birds, wild birds, and horses from similar regions were included. These selected samples (Table 1) were subjected to a different RNA extraction protocol to ensure the acquisition of high-quality starting material for WGS. Briefly, each organ homogenate suspension (250 µl) was lysed in 750 µl TRIzol™ LS Reagent (Invitrogen) or approximately 30 mg tissue material homogenized in 1 ml TRIzol™ reagent via TissueLyser II (Qiagen) with a 5 mm steel bead for 2 min at 30 Hz. After phase separation, the aqueous phase was processed using the Agencourt®

147 RNAdvance Tissue kit (Beckman Coulter) and the KingFisher Flex system (Thermo Fisher Scientific)
148 according to the manufacturer's instructions.

149 WGS of WNV was performed as described (Quick et al. 2017) with some modifications. Briefly, RNA
150 was reverse transcribed using the SuperScript™ IV First-Strand Synthesis System (Invitrogen) with
151 random hexamers. The cDNA was subjected to the WNV-specific multiplex PCR described in (Sikkema
152 et al. 2020). Using two different primer mixes (Table S1) and an AccuPrime™ *Taq* DNA Polymerase Kit
153 (Invitrogen), two multiplex PCR reactions were performed. Amplicons were purified with 1.8 volume
154 of Agencourt® AMPure XP beads (Beckman Coulter) and quantified using a NanoDrop™ ND1000
155 Spectrophotometer (Thermo Fisher Scientific). These two purified and quantified amplicon pools were
156 combined per sample in equal concentration (125 ng each) and the volume adjusted to 130 µl.
157 Fragmentation and library preparation steps were performed according to (Wylezich et al. 2018).
158 Quantified libraries (GeneRead DNA Library L Core Kit; QIAGEN) were sequenced using an Ion Torrent
159 S5 XL instrument with Ion 530 chips and respective reagents (Thermo Fisher Scientific) in 400 bp mode
160 according to the manufacturer's recommendations.

161 We verified the PCR-based sequencing using five WNV-positive samples from previous seasons (C1-C5;
162 Table S2) that had already been sequenced according to the validated approach described in (Wylezich
163 et al. 2018). Two previously completed libraries of C4 and C5 were enriched for WNV using MyBaits
164 (Wylezich et al. 2018; Wylezich et al. 2021) but still only yielded partial genome sequences. On the
165 contrary, the multiplex PCR-based approach generated complete coding sequences of all 5 test
166 samples, albeit with a truncated 3´ end (23-71 nucleotides). The sequences from both approaches were
167 100% identical for samples C1-C3 and showed a few differences for samples C4 and C5 (Table S2).
168 These results demonstrated that the multiplex PCR approach is suitable for reliable and sensitive WGS
169 of WNV, even from samples with low WNV concentration (up to C_q value 31.5).

170 Sample #26 (ED-I-258/20) had a genome region with a sequencing depth lower than 30, therefore
171 sequencing results were confirmed with Sanger sequencing. Briefly, cDNA from sample ED-I-258/20
172 was amplified using additional single-plex PCR assays (primer pairs: WNVUS1_30_LEFT and

WNVUS1_30_RIGHT_2, WNVUS1_30_LEFT_2 and WNVUS1_30_RIGHT). The amplicon was sequenced with a BigDye Terminator v1.1 Cycle Sequencing kit (Applied Biosystems™, Thermo Fisher Scientific) on a 3500 Genetic Analyzer Instrument (Applied Biosystems™, Thermo Fisher Scientific).

WNV genome sequences obtained in this study were submitted to the European Nucleotide Archive under the BioProject accession number PRJEB47687.

2.5 Datasets

We validated our workflow using two test datasets consisting of WNV complete coding sequences previously characterized and classified into different ranks below the species level. “Test dataset 1” (TD01) consists of 95 WNV whole-genome sequences characterized and classified into different lineages by Fall and colleagues (Fall et al. 2017). Notably, this study considered WNV clades 1a, 1b, 1c, 4a, and 4b/9 as distinct lineages. “Test dataset 2” (TD02) consists of 150 WNV whole-genome sequences allocated to three WNV clades and six WNV clade 1a clusters described by May and colleagues (May et al. 2011). We also combined the sequences from these two test datasets, and a sequence described as a member of the putative WNV clade 1a cluster 7 (Aguilera-Sepulveda et al. 2021). We referred to these sequences as “test dataset 3” (TD03). Available complete coding sequences of WNV lineage 2 and their metadata (e.g. sample collection year and country of origin) were retrieved from GenBank on 10th December, 2021. WNV lineage 2 dataset (WL2) consisted of WNV complete coding sequences from the database and sequences acquired in this study. Accession numbers of WNV sequences per dataset are summarized in Table S3. We also prepared versions of these datasets that excluded sequences with ≥10 ambiguous nucleotides or gaps, and duplicates.

2.6 *In-silico* analyses

2.6.1 Sequence assembly

Genome sequences were assembled from raw data using the Roche/454 genome Sequencer software suite v3.0 (Roche). Sequencing adapters and PCR primers were trimmed using the Newbler assembler prior to reference mapping. Initial reference-based mapping against WNV strain 1382/2018/Berlin/Ger

198 (MH986055.1) was done to generate a sample specific consensus sequence. These consensus
199 sequences were then employed as the reference for a second reference-based mapping per dataset.
200 The resulting genome sequences were visually inspected using the Geneious Prime® 2021.0.1 software
201 (Biomatters).

202 *2.6.2 WNV genome characterization and phylogenetic analyses*

203 Complete coding sequences from each dataset (TD01, TD02, TD03, WL2) were aligned using the
204 MUSCLE algorithm (Edgar 2004), and visually inspected using Geneious Prime® 2021.0.1.

205 *2.6.3 Maximum likelihood phylogenetic analysis*

206 The best-fitting nucleotide substitution model for each dataset was calculated using jModelTest 2.1.10
207 (Darriba et al. 2012). Maximum likelihood (ML) inference with the determined best substitution model
208 and ultrafast bootstrap option (Hoang et al. 2018; Minh et al. 2013) with 100,000 replicates was
209 performed using IQ-TREE 1.6.8 (Nguyen et al. 2015). ML phylogenetic trees were viewed using FigTree
210 software (v1.4.4, http://tree.bio.ed.ac.uk/software/figtree/).

211 *2.6.4 Bayesian phylogenetic analysis*

212 We subjected the dataset consisting of complete genome sequences belonging to the subclade 2.5.3
213 to the Bayesian Markov Chain Monte Carlo (MCMC) method implemented in the Beast package version
214 1.10.4 (Drummond and Rambaut 2007; Suchard et al. 2018). We performed regression analyses of the
215 root-to-tip genetic distance in the resulting ML trees against sampling years using TempEst (Rambaut
216 et al. 2016). The spatiotemporal dynamics of WNV and the time to most recent common ancestors
217 (MRCA) were co-estimated using best suited substitution model based on the jModelTesT 2 (Darriba
218 et al. 2012), optimal molecular clock model (relaxed uncorrelated lognormal) and best demographic
219 scenario (the Bayesian SkyGrid coalescent model), which will be explained below.

220 The optimal molecular clock model (strict or relaxed uncorrelated log normal) and tree prior (Constant,
221 Bayesian GMRF Skyride, or Bayesian Skygrid model) were selected based on the marginal likelihood
222 estimation path sampling and stepping stone sampling methods. The MCMC chain length was run until

223 convergence and sampled every 10^4 iterations. Convergence was evaluated by approximating the
224 effective sampling size (ESS) after a 10% burn-in using the Tracer software version 1.7.1, with ESS
225 values >> 200 accepted. The strength of the evidence against H_0 was evaluated according to Kass and
226 Raftery's (Kass and Raftery 1995) Bayes factor test as follows: Bayes factor (BF) 1-3 – weak, BF 3-20 –
227 positive, BF 20-150 – Strong, and >150 – very strong (comparison of each parameter summarized in
228 Table S4).

229 Phylogeographic analysis was performed using a discrete model attributing state characters
230 represented by the detection of location (country) of each strain and the Bayesian stochastic search
231 variable (BSSV) algorithm implemented in BEAST v1.10.4 (Suchard et al. 2018). TreeAnnotator v1.10.4
232 was employed to summarize the maximum clade credibility (MCC) tree after 10% burn-in and Figtree
233 software v1.4.4 was utilized to visualize the MCC tree. The branches of the trees were color-coded
234 based on the sample's geographic origin (country).

235 *2.6.5 Affinity propagation clustering (APC)-based workflow for sequence grouping*

236 We analyzed WNV complete coding sequences using a workflow comprising of the APC algorithm and
237 AHC included in the R package "apcluster" (Bodenhofer et al. 2011) implemented in R v4.1.2 and R
238 studio (v2021.09.1-372)(R Core Team 2021). The APC algorithm requires a dissimilarity matrix as input
239 for clustering. For each of the determined clusters, one entity is defined as the "best representative"
240 or the "cluster exemplar".

241 Using the Sequence Demarcation Tool (SDT; SDT_Linux64 v1.2) (Muhire et al. 2014), we calculated
242 pairwise global alignments of the coding sequences and from these alignments used the pairwise
243 nucleotide identities to calculate a dissimilarity matrix by subtracting the identities from 1.
244 Subsequently, to increase the robustness and discriminatory power of the APC, these dissimilarities
245 were squared and converted to negative values according to Fischer and colleagues (Fischer et al.
246 2018) in order to yield the suitable input data for the APC algorithm.

One major problem in clustering is finding the suitable number of clusters to subdivide the dataset into. To this end, Fischer and colleagues (Fischer et al. 2018) developed the "plateau method" to calculate the optimum number of clusters. The number of clusters generated by APC is determined by a parameter called input preference, which by default is set to 0.5. Using the AP clustering algorithm, the suitable "input preference range" from minimum (pmin) to maximum (pmax) can be calculated. For the plateau method, the number of clusters (z-value) is repeatedly determined in dependence of the input preference which is increased in equal steps through the preference range. Usually, with an increase of the input preference, the number of groups monotonously increases; if a reduction occurs, this is deemed a disturbance that leads to the termination of the calculations. Fischer and colleagues defined the best suited number of groups corresponding to the longest plateau that was observed (the same number of clusters observed consecutively for the highest number of iterations before a disturbance occurred). While in principle this was suitable, they nevertheless found that it was not optimal. Since there can be a monotonous increase of the group number without a disturbance occurring throughout the whole preference range, we tested using the last stable plateau as an alternative measure for the definition of the group number. The last stable plateau is defined as the last plateau without disturbance and with at least the set minimal length. For this calculation, we set the minimum number of iterations that make a plateau to 3. Finally, for the definition of the most suitable number of groups present in the input data, the following rules were applied: (i) if both the longest and the last stable plateau resulted in a cluster number higher than the default APC, use the default; (ii) else, if either or both of the plateaus result in values lower than the default, use the higher of the values to set the number of groups. This number of groups was then used to calculate the grouping of the input dataset using the function for AHC from the APC package. The described grouping was applied for the desired number of sub-grouping levels (ranks below the species level). The R code used for these calculations is available as supplemental material.

In order to test the impact of the number of steps and minimum number of iterations to use as the cut-off for definition of the last plateau for the determination of the group number, we used the

273 described test datasets. We ran all calculations with all possible combinations of different step
274 numbers (1,000; 2,000; 5,000; 10,000), minimum plateau lengths (sliding window size 1%, 0.5%, 0.25%,
275 0.1%, or 0.01% of the step number) and minimum group members to have as input for further sub-
276 grouping (5; 7; 10). In these tests, we found that the coherence of grouping by the described workflow
277 and the phylogenetic trees increased with the number of steps and with the reduction of the sliding
278 window size applied for plateau determination. Notably, with a fixed set of step number and sliding
279 window size, the impact of the minimal group size increases with the increasing size of the input
280 dataset. Since our initial tests showed that ambiguities in the sequences and to a lesser extent also
281 duplicated sequences negatively impact the grouping by the described workflow, we also tested the
282 different test datasets without duplicate sequences and sequences with ≥10 ambiguous nucleotides
283 or gaps. Here, we present results from datasets without sequences having ≥10 ambiguous nucleotides
284 or gaps, and only retained one representative for sequences sharing 100% nucleotide identity. Unless
285 indicated, the used parameter set for the presented results were 10,000 steps, sliding window
286 proportion resulting in sliding window length 3, and minimum group size 5.

287 ### *2.6.6 Proposal for WNV group designations*

288 Alongside our new workflow, we here propose to use a generic nomenclature based on a hierarchical
289 numbering system. This proposal is outlined in Figure 1. Based on the use of designations in the
290 literature, we propose to designate the levels within the species WNV descending from the species
291 through lineage, clade, subclade, cluster, and finally subcluster. The subclusters can additionally be
292 divided further, then carrying a letter as the suffix. The digits representing the different hierarchical
293 levels are separated by a "." (compare Figure 1). Here, we examined the grouping in different depths
294 as indicated for the respective analyses. With the lineage designations we followed the established
295 lineage numbering; hence, where necessary, lineage designations automatically assigned in the
296 calculations were replaced by the corresponding established designations.

2.6.7 Combination of the clustering workflow, phylogenetic analyses and geolocation

The assigned hierarchical levels of WNV sequences detected in Germany from 2018-20 were summarized per new phylogenetic group, collection year, and sample type (wild/captive bird, horse, mosquitoes, and humans). These were exported as a CSV file into the QGIS Desktop (v3.16.15).

3. Results and Discussion

Originally, the goal of this study was to provide an update on the WNV epizootic in Germany in 2020. However, we encountered significant problems in consistently allocating WNV sequences into different groups below the species rank, namely:

1) the lack of objective grouping due to undefined demarcation criteria for the splitting of sequences into groups, resulting in arbitrarily adjusted groupings, and
2) the missing common group designations below species level within the West Nile Virus species (and in general) that together with the used nomenclature, which often relies on geographical terms that due to the spread of the virus no longer fit, result in misleading designations.

3.1 Proposal for a hierarchical WNV nomenclature below the species level

To date, there is no commonly used system in the WNV research community for the definition and designation of virus groups below the species level. Rather, a substantial number of ways to define and terms to designate virus groups at different levels of a hierarchical system below the species are used. These are also different from what is used for other virus species and what is commonly understood (see Table 2).

The designations of the hierarchical levels *inter alia* include the terms “lineage”, “clade”, and “cluster” (Figure 2). However, the use of the labels to designate different levels of the hierarchical system is variable. The WNV research community especially uses the term “lineage” to describe a broader

hierarchical group consisting of clades and/or subclades, while in other virus species, such as severe acute respiratory syndrome coronavirus 2 (SARS-CoV-2) and rabies virus (RABV), the term "clade" defines a broader monophyletic group consisting of subclades and lineages (Campbell et al. 2022; Rambaut et al. 2020).

Moreover, beside the variable use of terms for the designation of hierarchical levels, the criteria used to define the groups are variable. For instance, Aguilera-Sepulveda et al. (2021); Barzon et al. (2015) and May et al. (2011) defined clusters found within WNV clade 1a as sequences belonging to a monophyletic group with a close phylogenetic relationship, with a common ancestor and fixed and unique amino acid substitutions. In another example, McMullen et al. (2013) defined four clades (clades 2a – 2d) based on nucleotide identities and monophyletic branching within the phylogenetic tree. However, the demarcation criteria regarding nucleotide identities or amino acid similarities for each clade were not clearly defined.

Likewise, the labels used to designate the groups are diverse. Often, groups are labelled according to their first geographic occurrence. Although geographic labels may provide epidemiological information regarding the origin of the WNV cases, these descriptive labels can cause misrepresentation. For instance, the geographic range of WNV cases designated to the Lombardy cluster, which consisted of WNV cases from Lombardy, Italy, as of 2015 (Barzon et al. 2015), is recently expanding. The Lombardy cluster now also includes WNV sequences from France and Spain (Aguilera-Sepulveda et al. 2022). Similarly, WNV clade 2d sequences from the European continent were designated according to the supposed region of the viruses' origins, like WNV sequences from Russia and Romania that were designated as the Eastern European lineage 2 WNV (EE, Figure 3) (Cotar et al. 2018; Ravagnan et al. 2015) or WNV sequences from Hungary, Austria, Greece, Serbia, and Italy that were put into the Central/Southern European lineage 2 WNV (C/SE, Figure 3) (Chaintoutis et al. 2019; Ziegler et al. 2020).

Due to the issues outlined above, we set out to design a novel unified system for the hierarchical organization of WNV (and other viruses) based on (I) an objective definition of subgroups (see paragraphs 2.6.5 and 3.2), (II) a defined set of names for the different nested hierarchical levels, and

(III) a system for group designations that does not rely on geographic or other names that can likely be subject to change. Although we acknowledge the importance of a universal designation below the species rank encompassing all virus species, we in part still followed the conventional designation of WNV sequences below the species rank to prevent any confusion. For the species *West Nile virus*, we define a term associated with a specific hierarchical level, as summarized in Table 2. We propose to use the following order of hierarchical groups based on increasing shared genetic identities within the group: lineages (highest level below the species, as commonly used in the WNV community, level 1), clade (level 2), subclade (level 3), cluster (level 4), and subcluster (level ≥ 5). Moreover, we propose to utilize a generic nomenclature for the defined groups based on a hierarchical numbering system to designate each group at different hierarchical ranks in a logical and standard manner (Table 2, column "Suggested Usage"). These generic labels also provide information regarding the hierarchical level through the number of decimal and/or alphabetical places included (compare Figure 1). Furthermore, these generic labels can be used continuously even when the group members do not share particular characteristics, such as geographic origin. Finally, we applied these proposals to WNV sequences from previously published studies and members of WNV lineage 2 available in the public database to compare our results with previous classifications.

3.2 Application of the developed grouping workflow yields reasonable groups

To address the grouping issues outlined above, we developed a workflow for objective clustering of sequences into different hierarchical groups below species level. This clustering workflow employs APC, which is a non-hierarchical mathematical clustering method, with AHC to split the dataset into groups. This workflow is based on the works of Fischer and colleagues (Fischer et al. 2018), who initially utilized APC to define objective clusters of RABV sequences. Their group also developed the plateau method to determine the number of clusters in a given dataset, typically a user-defined parameter required in clustering programs such as HierBAPS (Cheng et al. 2013), Cluster Picker (Ragonnet-Cronin et al. 2013), TreeCluster (Balaban et al. 2019), and PhyClip (Han et al. 2019). Furthermore, the workflow of Fischer and colleagues only requires pairwise identities between all pairs of virus sequences as input.

Overall, the method overcomes the need for inputting subjective criteria like number of clusters, the minimum number of sequences per cluster, or support thresholds for cluster allocation. While Fischer and colleagues successfully assigned RABV and *Francisella tularensis* isolates into reasonable objectively defined clusters (Busch et al. 2020; Fischer et al. 2018), the APC results were partly incongruent with the branching of a RABV phylogenetic tree. This incongruence is potentially caused by the non-hierarchical clustering properties of the APC algorithm in contrast to the phylogenetic analysis (Fischer et al. 2018), but could also be caused by an uncertainty of the suitable number of clusters present in the dataset. Therefore, to improve the workflow, we further developed the determination of the number of clusters and included AHC to determine the generated clusters. In order to define multiple hierarchical levels, the method was iteratively applied to subsets of the data corresponding to the subgroups of the preceding iteration, i.e. higher level in the hierarchy. For optimization of the parameters, we repetitively analyzed the described test datasets and compared the results with the grouping as described in the respective studies (Chaintoutis et al. 2019; McMullen et al. 2013; Ravagnan et al. 2015; Zehender et al. 2017; Ziegler et al. 2020). We found that the minimum number of sequences per group to be used as input for further subgrouping and the number of iterations used to define the plateau (the window size) had the major impact on the results. On the contrary, the overall number of iterations applied to determine the number of clusters only had less influence. The optimal parameters used for all subsequent analyses were the window size of 3 for the determination of the longest and last stable plateaus, respectively, and the group size of 5 that was necessary to further split the group. In order to ensure that the number of iterations did not limit the quality of the clustering, we used 10,000 iterations throughout.

We initially applied the developed workflow with the settings outlined in the previous paragraph to the test dataset TD03 for the definition of groups within the three proposed levels “lineage”, “clade”, and “subclade”. Figure 2 shows the result of grouping TD03. According to the used minimum size of a group to be used as input for further subdivision in the next lower hierarchical level, the grouping stopped at different levels of the hierarchy. Overall, the objective APC grouping coincides with groups

399 that would be defined when analyzing the tree visually. Most groups we found fit with the traditional
400 definition of a phylogenetic group being monophyletic. In case of the grouping result for TD03,
401 however, we received one subclade (1.3.5) that was not intuitively clear at the first glance at the tree
402 because it was not monophyletic (Figure 2; subclade 1.3.5). This subclade is split in two parts
403 (interspersed by subclades 1.3.7 and 1.3.8), which are in the graph connected with a dashed line with
404 arrows pointing inwards. This split is possible since our workflow mainly depends on the nucleotide
405 identities of pairwise aligned sequences but not on reconstructed hierarchical connections. Looking at
406 the tree in more detail, it becomes clear that the branch lengths between the three subclade members
407 are indeed quite short and therefore the grouping makes sense. Hence, we proceeded with the proof-
408 of-concept for the developed method.

409 ### *3.3 Proof-of-concept for the developed clustering workflow*

410 For the proof-of-concept, we compared our grouping results with published groupings. Using the
411 abovementioned parameters, we could reproduce the groupings of test datasets TD01 and TD02 as
412 published (Fall et al. 2017; May et al. 2011) (results not shown). For the combined dataset TD03, we
413 obtained the grouping shown in Figure 2. Both Fall and colleagues and Rizzoli and colleagues
414 categorized WNV lineages 1a, 1b, 1c, 4a, and 4b (4/9) as distinct and separate lineages (Fall et al. 2017)
415 (Rizzoli et al. 2015), while May and colleagues designated the same groups of sequences belonging as
416 clades 1a, 1b, and 1c which they further subdivided into clusters (May et al. 2011). As can be seen, the
417 objective grouping of the APC/AHC workflow overall coincides with the previously performed
418 groupings, albeit at different levels of the hierarchy and hence different labels. At the lineage level,
419 although lineages 1a, 1b, and 1c (Fall) and 4a and 4b (Fall), respectively, are fused together in one
420 group each by the APC/AHC workflow, the new defined lineages match those of Fall and colleagues
421 (Fall et al. 2017). At the next level (clade), our workflow divides the fused lineages into clades, with
422 lineage 4b (Fall et al. 2017) corresponding to clade 4.3 and lineage 4a (Fall et al. 2017) being subdivided
423 into clades 4.1 and 4.2. Likewise, lineages 1a, 1b, and 1c (Fall et al. 2017) correspond to clades 1.1 (1c),
424 1.2 (1b), and 1.3 (1a). At the subclade level of our proposed nomenclature, the clusters that May et al.

(2011) defined within lineage 1a match our subclades quite well: the members of the cluster 1a/1 (May et al. 2011) are comprised within the subclades 1.3.1 and 1.3.2; sequences of cluster 1a/2 are comprised in subclade 1.3.8; 1a/3 and 1a/4 correspond with subclades 1.3.4 and 1.3.3, respectively; finally, clusters 1a/5 and 1a/6 are combined into subclade 1.3.5. Notably, subclade 1.3.5 is not a monophyletic group but in the phylogenetic tree all descend from the same branch and their branch lengths are very short. Therefore, the co-allocation by APC/AHC is congruent with the minor distances that are visible in the phylogenetic tree. In summary, although in detail there are a few differences, overall, the developed objective grouping by APC/AHC yields meaningful and reliable groupings.

In addition to the above proof of concept study for the separation of WNV of all lineages into the different hierarchical levels (lineages, clades, and subclades), we analyzed the WNV lineage 2 complete coding sequences available in the INSDC databases. As stated above for the first analysis, the grouping we received overall fit well with what is seen intuitively in the tree. Usually, the observed polyphyletic interspersed groups, e.g., clades 2.2 and 2.5 in Figure 3, which are in part associated with low ultrafast bootstrap values in the tree (according to the IQ-Tree documentation, only values above 95 % indicate trustworthy clades (Minh et al. 2022)) are resolved at the next lower grouping level (in this example at the subclade level). Here, clade 2.2 (Figure 3) is a polyphyletic group comprising five sequences, which are at the subclade level separated into subclades 2.2.1 and 2.2.2. This interspersed grouping at the clade level, which occurs in the APC step based on the pairwise identities, cannot be resolved using AHC. This incongruency is due to the inherent non-hierarchical characteristics of the APC, as described by Fischer and colleagues (2018). Similarly, in the deeper grouping of subclade 2.5.3 sequences, subcluster 2.5.3.4.3a includes WNV sequences that are interspersed in the ML and MCC trees (Figure 4). This subcluster formed a paraphyletic group in both ML and MCC trees, and demonstrated low ultrafast bootstrap values (<80%) and posterior probability values (<0.6), respectively.

The discussed topology in phylogenetic trees depicts the so-called “supercluster”, wherein divergent subgroups are nested within a more extensive cluster structure (Han et al. 2019). Therefore, in combination with phylogenetic trees our grouping workflow can also provide insights regarding the

source-sink ecological dynamics of WNV lineage 2 in Europe. This dynamic has been previously discussed in the phylogeographic and phylodynamic analyses of Zehender et al. (2017) and Ziegler et al. (2020). Specifically, cluster 2.5.3.4 may represent the putative source of the WNV population that gives rise to its subgroups, reflecting the trajectory and divergence of variants (Han et al. 2019). In parallel, members of cluster 2.5.3.4 were detected in locations described as "radiation centers or sources" of WNV lineage 2 migration in Europe (e.g., Hungary and Austria). Furthermore, members of other WNV clusters were detected in areas described as "receiving areas or sinks" of WNV migration, such as Greece (cluster 2.5.3.3).

To further verify the workflow, we compared our grouping with previously published results of McMullen et al. (2013), Ravagnan et al. (2015), Zehender et al. (2017), Chaintoutis et al. (2019) and Ziegler et al. (2020). Noteworthy, all studies that were available for comparison only included partial sets of the sequences that we included here. The comparison of the results of the objective APC/AHC grouping and the clades defined by McMullen (McMullen et al. 2013) shows that there are two main differences between both: (i) McMullen's clade 2b is disrupted into clades 2.3 and 2.4 in our grouping; this is likely caused by the inclusion of the 2020 sequence from Namibia (MW383507), which forms clade 2.4 together with the 1958 South African sequence (HM147822) that was included in McMullen's clade 2b; (ii) the sequences comprised in McMullen's clade 2d were now put into clade 2.5, except for 1990 Senegal (DQ318019) and 1937 Uganda (NC_001563) that form clade 2.2 together with one 1988 sequence from Madagascar (HM147823). These two deviations show the expectable effect of addition of sequences on tree topology and sequence grouping. The comparison between the groupings of Ravagnan and colleagues (Ravagnan et al. 2015) and ours shows that the virus group designated "Eastern European lineage 2 WNV" (labelled EE in Figure 3) coincides with our subclade 2.5.4 and those of the "Central/Southern European lineage 2 WNV" (labelled C/SE in Figure 3) are all grouped into subclade 2.5.3. In the studies of Zehender et al. (2017), Chaintoutis et al. (2019) and Ziegler et al. (2020), viruses belonging to Ravagnan's C/SE lineage 2 WNV (Ravagnan et al. 2015) were subdivided into two groups. These were labelled clade A (Zehender) or Central and Eastern European clade (CEC;

Ziegler; Chaintoutis) and clade B (Zehender) or Southeastern European clade (SEEC; Ziegler; Chaintoutis), respectively. Using our APC/AHC workflow, they are grouped together in subclade 2.5.3. At the next hierarchical level (cluster), with a single exception (LR743454, Germany 2019, cluster 2.5.3.2), clade A/CEC is completely comprised within cluster 2.5.3.4. Likewise, clade B / SEEC is fully comprised in cluster 2.5.3.3, except for the two sequences from Hungary 2014 (KT359349) and Serbia 2010 (KC496016). Interestingly, cluster 2.5.3.1 comprises only a single WNV sequence from Austria (KP780840) that has not been included in previous phylogenetic studies (Chaintoutis et al. 2019; Ziegler et al. 2020) since it was considered an outlier based on its temporal signal relative to other WNV subclade 2.5.3 sequences. This sequence also showed the lowest pairwise nucleotide identities among members of subclade 2.5.3. Noteworthy, Ziegler and colleagues highlighted that LR743454 formed its own distinct subclade within the CEC. In our analysis, this sequence received two companions, altogether forming cluster 2.5.3.2.

Taken together, the presented comparisons between published studies and the grouping obtained by application of the newly developed APC/AHC workflow show that our objective workflow reliably puts sequences into meaningful groups.

3.4 WNV circulation in Germany extended in space and species

In 2020, we detected 65 birds (captive = 33 and wild = 32) and 22 horses that tested positive for WNV in Germany (diagnosed between July 14 and October 20 and two retrospective cases from 2021). All but one WNV-positive bird succumbed to infection (Table 1; #44). The number of notifiable cases of WNV in birds and horses in 2020 is similar to the previous year, particularly in regions with the highest WNV activity i.e., Berlin, Saxony, and Saxony-Anhalt (Figure 5) (Ziegler et al. 2020). However, we observed an increasing number of WNV-cases in Brandenburg, Thuringia, and Lower Saxony. All WNV-positive birds and horses detected in 2020 were found in federal states which also reported WNV cases in 2018 and 2019 (Figures 5 and S1) except for a new WNV-case detected in Lower Saxony. Notably, all 22 probable autochthonous human WNV cases in 2020 occurred in these federal states (Berlin = 7; Saxony = 11; Saxony Anhalt = 4) (European Centre for Disease Prevention and Control 2020; Frank et

al. 2022; Pietsch et al. 2020). Therefore, this kind of WNV surveillance in both wildlife and captive animals could provide an early warning for autochthonous WNV-infection in humans in Germany. Hence, reports of WNV infection in birds and horses in an area must be provided promptly (e.g., updates of FLI websites) to advise the medical community and the public regarding a potential risk of WNV-infection in specific regions in Germany, as well as the risks in blood transfusion and organ transplantation safety. Although vaccines against WNV disease in humans are still under development (Ulbert 2019), clinicians must be aware of the potential presence of WNV circulation in the local region to reach a correct diagnosis since WNV diagnostics is not routinely performed in Germany (Schneider et al. 2021).

Here we report the first case of a WNV-infection in Lower Saxony, where a horse with WNV-specific IgM antibodies was detected in the Helmstedt district, and the first reported cases of WNV-infected birds in Thuringia, particularly in the districts of Erfurt and Gera (Figures 5 and S1). We also reported the first cases of WNV-infection in three districts in Brandenburg (i.e., Teltow-Fläming, Barnim and Dahme-Spreewald) and in one district in Saxony-Anhalt (Börde) (Figure S1). Areas with reported WNV-infection match with areas with high average temperatures (>20°C), lower average precipitation (≤250 mm), and lower average climatic water balance (-150 – 50 mm) in summer 2020 (Figure S2) (Deutscher Wetterdienst 2020). Higher average temperatures over several days may increase the risks of WNV transmission through mosquito vectors (Holicki et al. 2020). The higher average temperatures in these areas probably caused the epizootic emergence of WNV by shortening the extrinsic incubation period (EIP) in local mosquito populations. Furthermore, WNV activity is more likely to increase during drought than during rainy periods (Paull et al. 2017). It is also possible that the declining water sources force the avian reservoir hosts to aggregate, increasing the probability of contact between birds and mosquitoes and WNV transmission (Paull et al. 2017). However, we did not detect the re-emergence of WNV in Hamburg, and in two districts in Brandenburg (Ostprignitz-Ruppin and Havelland) in 2020, despite the observed higher average temperatures (>20 °C) and lower average precipitations (126-200 mm) in summer 2020.

We also detected WNV infections in 21 different bird species from six taxonomic orders (Table 3). The majority of WNV-infected avian species are classified as birds of prey (order *Accipitriformes*, 29%), followed by songbirds (order *Passeriformes*, 26%), captive flamingos (order *Phoenicopteriformes*, 23%) and owls (order *Strigiformes*, 17%). Most of the WNV-infected bird species in 2020 were also reported in an earlier study (Ziegler et al. 2020), except for the alpine chough *(Pyrrhocorax graculus*), Bohemian waxwing *(Bombycilla garrulus)*, and golden eagle (*Aquila chrysaetos*). However, all three species belong to taxonomic orders that were already described before to be repeatedly affected by WNV (*Passeriformes* and *Accipitriformes*) (Michel et al. 2018; Michel et al. 2019). Notably, the golden eagle from Brandenburg (#44) is the only reported case in 2020 that recovered from WNV-infection (Table 1).

3.5 Update on the WNV situation in Germany, 2020

After we had validated the workflow, we analyzed the ongoing WNV epizootic in Germany using this tool. The result of grouping sequences that belong to subclade 2.5.3, to which all viruses circulating in Germany until 2020 belong, is shown in Figure 4. As can be seen, subclade 2.5.3 can be further subdivided into the four clusters 2.5.3.1, 2.5.3.2, 2.5.3.3, and 2.5.3.4. Interestingly, cluster 2.5.3.1 only comprises the beforementioned Austrian sequence KP780840 that was previously deemed an outlier and therefore disregarded in previous analyses. Cluster 2.5.3.2, which can due to the group size restriction also not be further subdivided, consists of three German sequences (LR743454 from 2019 and #32 and #37 from 2020), also mentioned above. On the contrary, clusters 2.5.3.3 and 2.5.3.4 can be further subdivided into multiple subclusters each. Although to a large extent the detected subclusters comprise sequences from individual countries, they are clearly not geographically homogenous, highlighting the problem of geographic criteria for the designation of phylogenetic groups. For instance, subcluster 2.5.3.4.3b mainly comprises sequences from Italy but also 2 from France and 1 sequence of a case imported to Germany (MH910045). Likewise, subcluster 2.5.3.4.3c, into which the majority of WNV sequences from Germany were grouped, also comprises sequences from Slovakia (n=2), Austria (n=5), and the Czech Republic (n=2).

As summarized in Figures 6 and 7, sequences from WNV circulating in Germany from 2018-20 were allocated to cluster 2.5.3.2 and subclusters 2.5.3.4.3a and 2.5.3.4.3c, respectively. A sequence of cluster 2.5.3.2 was first detected in 2019 (LR743454) and previously formed an outlier (Ziegler 2020) but now two additional viruses of this cluster were detected (ED-I-228-20 - #32, ED-I-210-20 - #37) (Figure 6). The MRCA of WNV in cluster 2.5.3.2 (see Figure 4) was estimated to have existed around 2018 (95% highest posterior density or 95% HPD: 2017- 2019; Bayesian posterior probabilities or pp: 100%). Unlike viruses of cluster 2.5.3.2, viruses of subcluster 2.5.3.4.3a were only detected in 2018 (ED-I-127-18 – C5) and 2019 (LR743431, LR743448), but not in 2020 (Figure 6). Given the available WNV genome sequences, we cannot confirm whether these minor genotypes (cluster 2.5.3.2 and subcluster 2.5.3.4.3a) have successfully overwintered or been introduced to Germany in separate events. Furthermore, we may have missed these minor WNV clusters and subclusters as we could not sequence all WNV-positive cases from 2018-20 (Table 1; #45). For instance, most horse samples are serologically WNV IgM positive but WNV-RNA negative, preventing the successful sequencing of WNV genomes. Moreover, organ materials from small passerines were often depleted after necessary routine diagnostics at the regional veterinary laboratories for other relevant avian viruses or after confirmatory diagnostics at the national reference laboratory at the FLI. In some cases, simply the sample quality and/or quantity prevents from generating the genome sequences, despite the use of the WNV multiplex-PCR-based HTS approach (Sikkema et al. 2020).

Beside the above mentioned two minor groups, the vast majority of WNV circulating in Germany were allocated to subcluster 2.5.3.4.3c, which comprises all sequences previously allocated to the EGC plus additional sequences, inter alia two previously defined minor subclades comprising sequences LR743422 and LR743437/LR743434 (Ziegler et al. 2020). The EGC, which was the dominant genotype that circulated in Germany from 2018-19, was characterized by a unique non-synonymous mutation ($Lys_{2114}Arg$) located within the NS3 encoding genome region (noteworthy, LR743444 and LR743425 were previously designated into the EGC but do not harbor this mutation). This mutation no longer is a marker of the respective group (subcluster 2.5.3.4.3c) which also comprises sequences without that

specific mutation. Overall, the grouping we now observed (one major subclade and two minor (sub)clusters agrees with our previous WNV report, wherein we detected six distinct "subclades" circulating in Germany in 2018 and 2019 (Ziegler et al. 2020).

We estimated that the MRCA of the monophyletic branch consisting of subcluster 2.5.3.4.3c sequences existed around 2010 (95% HPD: 2008–2011; pp: 100%). Despite the fact that the vast majority of the 2.5.3.4.3c sequences are from Germany, it appears highly unlikely that the ancestors of that subcluster evolved in Germany, as confirmed WNV-positive cases in Germany were only detected from 2018 onwards by the extensive arbovirus monitoring performed in the country since 2011 (Michel et al. 2019; Ziegler et al. 2022). Rather, given that (i) the estimated MRCA of the EGC coincided with large reported outbreaks in eastern and southeastern Europe (Aberle et al. 2018; Jungbauer et al. 2015; Kolodziejek et al. 2015; Kolodziejek et al. 2018; Rudolf et al. 2014; Sedlak et al. 2014; Vlckova et al. 2015) and (ii) WNV complete genomes are not available from neighboring countries, we cannot determine where this subcluster diverged. Therefore, we hypothesize that members of the EGC were more likely introduced to Germany from neighboring countries in separate events and in a later time than its estimated MRCA.

While we detected subcluster 2.5.3.4.3c all over the WNV affected regions in Germany from 2018 until 2020, making it the dominating subcluster, viruses of (sub)cluster 2.5.3.2 and 2.5.3.4.3a were both in time and space restricted and of minor impact for the ongoing epizootic (Figures 6 and 7). Like with the sporadic occurrence of the aforementioned two (sub)clusters, there are also regions within Germany where WNV occurrence is only sporadic (regardless of the virus' phylogenetic group). Namely, we detected WNV infected wild birds in Rostock, Mecklenburg-Western Pomerania in 2018 (n=1) and in Hamburg (n=1), Havelland, Brandenburg (n=1) in 2019. However, in these areas in the succeeding years, WNV activity was not reported.

As in the preceding years, in 2020, except for two cases in which viruses of cluster 2.5.3.2 were detected, all other viruses were grouped into subcluster 2.5.3.4.3c, and in the same cities and districts as before (Figure 7). In addition, viruses of subcluster 2.5.3.4.3c were detected in three districts in

607 Thuringia. These observations suggest that viruses of subcluster 2.5.3.4.3c successfully established in
608 local avian and mosquito populations in the affected regions, namely in Berlin, Saxony (particularly
609 within Leipzig and neighboring areas) and Saxony-Anhalt, which led to the endemic circulation of WNV
610 in these areas in 2020. We also observed the continuous geographic expansion of WNV belonging to
611 subcluster 2.5.3.4.3c from 2018 to 2020; however, only time will tell whether members of this
612 subcluster successfully overwinter and establish themselves in these newly affected areas. In 2021,
613 however, WNV cases in birds and horses were predominantly reported in Berlin, with a few additional
614 WNV-cases reported in Saxony, Saxony-Anhalt, and Brandenburg (FLI report).

615 WNV sequences within subcluster 2.5.3.4.3c from Germany were acquired from mosquito pools (n=2),
616 horses (n=2) and different bird species (n=78) belonging to seven taxonomic orders. Complete coding
617 sequences from five human WNV cases reported from 2019 (n=1) to 2020 (n=4) were also allocated
618 into WNV subcluster 2.5.3.4.3c (Figure 6). We excluded a few human WNV cases where either only a
619 partial genome sequence (n=2) (Pietsch et al. 2020; Ziegler et al. 2020) or no sequence information at
620 all (n=3) (Ziegler et al. 2020) was available. These WNV cases did not meet the required criteria for the
621 APC/AHC grouping, i.e., WNV complete coding sequences with <10 nucleotide gaps or ambiguities. As
622 expected, the available partial WNV genome sequences of the two human cases (MN794936,
623 MW142225) had the highest sequence identities with members of the subcluster 2.5.3.4.3c. In
624 addition, recently published complete coding sequences (MZ964751.1, MZ964752.1, MZ964753.1)
625 from three human WNV cases reported in 2021 (Schneider et al. 2021) have the highest sequence
626 identities with members of subcluster 2.5.3.4.3c. Therefore, as of writing, only members of subcluster
627 2.5.3.4.3c have been reported to cause WNV infection in humans in Germany. Members of subcluster
628 2.5.3.4.3a, likewise detected in Germany, have previously been reported to cause human WNV-
629 infection in other countries, i.e. Austria (Kolodziejek et al. 2015; Kolodziejek et al. 2018). The higher
630 spread and frequency of subcluster 2.5.3.4.3c in Germany are the likely cause for it being the sole
631 subcluster so far associated with human WNV cases reported in Germany.

Here, we also obtained the complete coding sequence of WNV detected in a horse from 2018 (C5), grouping in subcluster 2.5.3.4.3a (Figures 4 and 7). Viruses of subcluster 2.5.3.4.3a are found widespread across Europe over a long period of time, e.g., in Italy (2011), Austria (2015-2016), the Czech Republic (2013), Slovakia (2013), Slovenia (2018), Germany (2018-2019), and the Netherlands (2020) (Figure 4). Noteworthy, we did not find any member of this subcluster among the sequenced WNV cases in 2020. Still, we cannot directly conclude that its absence in 2020 was due to a failed establishment in Germany since we were not successful in generating sequences from all 65 WNV PCR-positive birds from the 2020 season. The MRCA of WNV MW036634, detected in a Culex mosquito pool collected in Utrecht, the Netherlands, in 2020 (Sikkema et al. 2020) and LR743448 (collected in Cottbus, Brandenburg, Germany in 2019) was predicted to exist around 2013 (HPD 95%: 2011-2015 and pp: 35%) (Figure 4). However, these WNV cases from Cottbus and Utrecht were detected >600 km apart within a short period. Given the large distance between Utrecht and Cottbus together with the ubiquitous distribution of subcluster 2.5.3.4.3a in Europe, we suspect that these two WNV cases might be independent of each other, although they are the closest known relatives. Due to the greater distances between the Netherlands and those regions of Europe where related WNV were previously detected, we hypothesize that different modes of WNV dispersal other than bird migration may have played a role to the WNV introduction in the Netherlands. For instance, the translocation of WNV-infected mosquitoes inside vehicles (planes, ships, automobiles) may have occurred as described for different mosquito species (Bakran-Lebl et al. 2021; Brown et al. 2012; Eritja et al. 2017; Ronca et al. 2021).

Conclusions

Here, we introduced a structured and unbiased clustering workflow to systematically allocate WNV complete coding sequences to at least six hierarchical groups below the species level: **lineages, clades, subclades, clusters,** and **subclusters**. In addition, we propose a generic hierarchical decimal numbering system designating each group below species rank. We successfully applied the method to allocate

WNVs into groups below the species level and this workflow can also be applied to classify other virus species into hierarchical subgroups. Our workflow only requires a matrix of pairwise sequence identities as input. Essential parameters (e.g. number of clusters, threshold, etc.) are entirely decided by the mathematical algorithm, thus removing subjective input from users. Furthermore, the results of our workflow can be combined with different analyses, such as the classical phylogenetic ML tree and the time-scaled MCC tree.

Our analyses revealed that subcluster 2.5.3.4.3c was the predominant WNV subcluster circulating in Germany from 2018-20, accompanied by co-circulating minor WNV (sub)clusters. This finding indicates that the WNV genetic diversity in Germany is primarily influenced by the successful establishment, enzootic maintenance and expansion of subcluster 2.5.3.4.3c, possibly supplemented with continuous incursion and potential overwintering of WNV of other (sub)clusters. These other (sub)clusters detected in Germany overlapped in space and time with the dominant subcluster 2.5.3.4.3c. The minor groups were found in both wild and captive birds, as well as in horses. Therefore, to obtain the full picture of WNV circulation, it will be necessary to obtain whole-genome sequences from all WNV-cases whenever possible, to ensure that also minorities are found.

Since all human WNV cases in 2020 occurred in WNV hot spot areas, our study affirmed the importance of birds and horses as sentinels for human WNV-infections. Thus, information dissemination regarding WNV-infections should be conducted among healthcare and veterinary workers and the greater public. Furthermore, we recommend that horses located in these WNV hotspot areas and nearby regions be vaccinated against WNV according to the recommendations of the Standing Committee on Vaccination for Veterinary Medicine in Germany (StIKo Vet).

Acknowledgements

We are grateful to Patrick Zitzow, Cornelia Steffen, Katja Wittig, and Katrin Schwabe for excellent technical assistance. We are indebted to Dr. Susanne Fischer for the significant input regarding affinity

683 propagation clustering. We thank Sabine Bock (Berlin-Brandenburg State Laboratory, Frankfurt
684 (Oder)), Kerstin Albrecht (State Institute for Consumer Protection of Saxony-Anhalt, Department of
685 Veterinary Medicine, Stendal), Andrea Konrath (Saxon State Laboratory of Health and Veterinary
686 Affairs, Leipzig), Aemero Muluneh (Saxon State Laboratory of Health and Veterinary Affairs, Dresden),
687 Timo Siempelkamp (Thuringia Office for Consumer Protection, Bad Langensalza), Michael Sieg
688 (Institute of Virology, Faculty of Veterinary Medicine, Leipzig University, Leipzig), Claudia Szentiks
689 (Leibniz Institute for Zoo and Wildlife Research, Berlin), Dominik Fischer (Clinic for Birds, Reptiles,
690 Amphibians and Fish, Justus Liebig University Giessen, Giessen), Claudia Sauerwald (Landesbetrieb
691 Hessisches Landeslabor, Veterinary Virology and Molecular Biology, Gießen) and the other colleagues
692 of the veterinary authorities and veterinary laboratories of the federal states for the supply of the
693 samples and we are very grateful for the continuous support. Furthermore, we thank the staff of the
694 different bird clinics, rehabilitation centers, zoological gardens and “Tierparks” of Germany as partners
695 in the nation-wide wild bird surveillance network for zoonotic arthropod-borne viruses, which
696 collected and sent samples for the present study. Furthermore, we want to thank Patrick Wysocki and
697 Daike Lehnau (Institute of Epidemiology, FLI, Greifswald-Insel Riems) for their help by producing the
698 epidemiological datasets and Jacqueline King (Institute of Diagnostic Virology, FLI, Greifswald-Insel
699 Riems) for proofreading the manuscript.

700 This work was funded by European Union’s Horizon 2020 research and innovation program under the
701 Marie Skłodowska-Curie Actions grant agreement no. 721367 (HONOURs) and in part by the EU
702 Horizon 2020 program grant agreement no. 874735 (VEO) and by the German Federal Ministry of Food
703 and Agriculture (BMEL) through the Federal Office for Agriculture and Food (BLE), grant number
704 2819113919 (CuliFo2) as well as by the German Center for Infection Research (DZIF) under project
705 number TTU 01.804 (WBA-Zoo), and by the Federal Ministry of Education and Research within the
706 research consortium ‘‘ZooBoCo” (Grant No. 01KI1722A).

707

Data availability

The nucleotide sequences from this study are available from the INSDC databases study accession PRJEB47687.

References

Aberle, S. W., et al. (2018), 'Increase in human West Nile and Usutu virus infections, Austria, 2018', *Eurosurveillance,* 23 (43), 7-12.

Aguilera-Sepulveda, P., et al. (2021), 'A new cluster of West Nile virus lineage 1 isolated from a northern goshawk in Spain', *Transboundary and Emergerging Disease*.

Aguilera-Sepulveda, P., et al. (2022), 'West Nile Virus Lineage 2 Spreads Westwards in Europe and Overwinters in North-Eastern Spain (2017-2020)', *Viruses-Basel,* 14 (3).

Anez, G., et al. (2013), 'Evolutionary dynamics of West Nile virus in the United States, 1999-2011: phylogeny, selection pressure and evolutionary time-scale analysis', *PLoS Neglected Tropical Diseases,* 7 (5), e2245.

Bakran-Lebl, K., et al. (2021), 'Diversity of West Nile and Usutu virus strains in mosquitoes at an international airport in Austria', *Transboundary and Emerging Diseases*, 1-14.

Balaban, M., et al. (2019), 'TreeCluster: Clustering biological sequences using phylogenetic trees', *Plos One,* 14 (8), e0221068.

Bardos, V., et al. (1959), 'Neutralizing antibodies against some neurotropic viruses determined in human sera in Albania', *Journal of Hygiene, Epidemiology, Microbiology and Immunology,* 3 (3), 277-82.

Barzon, L., et al. (2015), 'Phylogenetic characterization of Central/Southern European lineage 2 West Nile virus: analysis of human outbreaks in Italy and Greece, 2013-2014', *Clinical Microbiology and Infection,* 21 (12), 1122.e1-22.e10.

Bodenhofer, U., Kothmeier, A., and Hochreiter, S. (2011), 'APCluster: an R package for affinity propagation clustering', *Bioinformatics,* 27 (17), 2463-64.

Brown, E. B. E., et al. (2012), 'Assessing the Risks of West Nile Virus-Infected Mosquitoes from Transatlantic Aircraft: Implications for Disease Emergence in the United Kingdom', *Vector-Borne and Zoonotic Diseases,* 12 (4), 310-20.

Busch, A., et al. (2020), 'Using affinity propagation clustering for identifying bacterial clades and subclades with whole-genome sequences of Francisella tularensis', *Plos Neglected Tropical Diseases,* 14 (9), e0008018.

Camp, J. V. and Nowotny, N. (2020), 'The knowns and unknowns of West Nile virus in Europe: what did we learn from the 2018 outbreak?', *Expert Review of Anti-Infective Therapy,* 18 (2), 145-54.

Campbell, K., et al. (2022), 'Making genomic surveillance deliver: A lineage classification and nomenclature system to inform rabies elimination', *PLoS Pathog,* 18 (5), e1010023.

Cellinese, N., Baum, D. A., and Mishler, B. D. (2012), 'Species and phylogenetic nomenclature', *Syst Biol,* 61 (5), 885-91.

Chaintoutis, S. C., et al. (2019), 'Evolutionary dynamics of lineage 2 West Nile virus in Europe, 2004-2018: Phylogeny, selection pressure and phylogeography', *Molecular Phylogenetics and Evolution,* 141, 106617.

Cheng, L., et al. (2013), 'Hierarchical and Spatially Explicit Clustering of DNA Sequences with BAPS Software', *Molecular Biology and Evolution,* 30 (5), 1224-28.

Cotar, A. I., et al. (2018), 'West Nile virus lineage 2 in Romania, 2015-2016: co-circulation and strain replacement', *Parasites & Vectors,* 11 (562).

Darriba, D., et al. (2012), 'jModelTest 2: more models, new heuristics and parallel computing', *Nature Methods,* 9 (8), 772-72.

Davis, C. T., et al. (2005), 'Phylogenetic analysis of North American West Nile virus isolates, 2001-2004: evidence for the emergence of a dominant genotype', *Virology,* 342 (2), 252-65.

Deutscher Wetterdienst (2021), 'Climatological maps of Germany', <https://www.dwd.de/EN/ourservices/klimakartendeutschland/klimakartendeutschland.html?nn=495490>, accessed 15.07.2021.

Di Giallonardo, F., et al. (2016), 'Fluid Spatial Dynamics of West Nile Virus in the United States: Rapid Spread in a Permissive Host Environment', *Journal of Virology,* 90 (2), 862-72.

Drummond, A. J. and Rambaut, A. (2007), 'BEAST: Bayesian evolutionary analysis by sampling trees', *BMC Evolutionary Biology,* 7, 214.

Edgar, R. C. (2004), 'MUSCLE: a multiple sequence alignment method with reduced time and space complexity', *BMC Bioinformatics,* 5 (1), 113.

Eiden, Martin, et al. (2010), 'Two new real-time quantitative reverse transcription polymerase chain reaction assays with unique target sites for the specific and sensitive detection of lineages 1 and 2 West Nile virus strains', *Journal of Veterinary Diagnostic Investgation,* 22 (5), 748–53

Eritja, R., et al. (2017), 'Direct Evidence of Adult Aedes albopictus Dispersal by Car', *Scientific Reports,* 7 (1).

European Centre for Disease Prevention and Control (2019), 'West Nile virus infection', *ECDC: Annual epidemiological report for 2018* (Stockholm: ECDC).

--- (2022), 'West Nile virus in Europe in 2020 - human cases, updated 19 November', <https://www.ecdc.europa.eu/en/publications-data/west-nile-virus-europe-2020-human-cases-updated-19-november>, accessed 24.02.2022.

--- (2021), 'Surveillance Atlas of Infectious Diseases', <http://atlas.ecdc.europa.eu/public/index.aspx?Dataset=27&HealthTopic=60>, accessed 14.07.2021.

Fall, G., et al. (2017), 'Biological and phylogenetic characteristics of West African lineages of West Nile', *Plos Neglected Tropical Diseases,* 11 (11), e0006078.

Fischer, S., et al. (2018), 'Defining objective clusters for rabies virus sequences using affinity propagation clustering', *Plos Neglected Tropical Diseases,* 12 (1), e0006182.

Frank, C., et al. (2022), 'West Nile Virus in Germany: An Emerging Infection and Its Relevance for Transfusion Safety', *Transfusion Medicine and Hemotherapy*.

Frey, B. J. and Dueck, D. (2007), 'Clustering by passing messages between data points', *Science,* 315 (5814), 972-76.

Goya, S., et al. (2020), 'Toward unified molecular surveillance of RSV: A proposal for genotype definition', *Influenza Other Respir Viruses,* 14 (3), 274-85.

Hadfield, J., et al. (2019), 'Twenty years of West Nile virus spread and evolution in the Americas visualized by Nextstrain', *Plos Pathogens,* 15 (10), e1008042.

Han, A. X., et al. (2019), 'Phylogenetic Clustering by Linear Integer Programming (PhyCLIP)', *Molecular Biology and Evolution,* 36 (7), 1580-95.

Hoang, D. T., et al. (2018), 'UFBoot2: Improving the Ultrafast Bootstrap Approximation', *Molecular Biology and Evolution,* 35 (2), 518-22.

Holicki, C. M., et al. (2020), 'West Nile Virus Lineage 2 Vector Competence of Indigenous Culex and Aedes Mosquitoes from Germany at Temperate Climate Conditions', *Viruses,* 12 (5).

ICTV (2022), 'Genus: Flavivirus', *The ICTV Report on Virus Classification and Taxon Nomenclature* (updated October 2020) <https://talk.ictvonline.org/ictv-reports/ictv_online_report/positive-sense-rna-viruses/w/flaviviridae>, accessed 25.02.2022.

Jungbauer, C., et al. (2015), 'West Nile virus lineage 2 infection in a blood donor from Vienna, Austria, August 2014', *Journal of Clinical Virology,* 64, 16-19.

Kampen, H., et al. (2020), 'West Nile Virus Mosquito Vectors (Diptera: Culicidae) in Germany', *Viruses,* 12 (5), 493.

Kass, Robert E. and Raftery, Adrian E. (1995), 'Bayes factor and model uncertainty.', *Journal of the American Statistical Association,* 90 (430), 773-95.

Kolodziejek, J., et al. (2014), 'The Complete Sequence of a West Nile Virus Lineage 2 Strain Detected in a Hyalomma marginatum marginatum Tick Collected from a Song Thrush (Turdus

809 philomelos) in Eastern Romania in 2013 Revealed Closest Genetic Relationship to Strain
810 Volgograd 2007', *Plos One,* 9 (10), e109905.
811 Kolodziejek, J., et al. (2015), 'West Nile Virus Positive Blood Donation and Subsequent Entomological
812 Investigation, Austria, 2014', *Plos One,* 10 (5).
813 Kolodziejek, J., et al. (2018), 'Integrated analysis of human-animal-vector surveillance: West Nile virus
814 infections in Austria, 2015-2016', *Emerging Microbes & Infections,* 7 (1), 1-15.
815 Kuno, Goro, et al. (1998), 'Phylogeny of the Genus *Flavivirus*', *Journal of Virology,* 72 (1), 73-83.
816 Mann, B. R., et al. (2013), 'Molecular Epidemiology and Evolution of West Nile Virus in North
817 America', *International Journal of Environmental Research and Public Health,* 10 (10), 5111-
818 29.
819 May, F. J., et al. (2011), 'Phylogeography of West Nile Virus: from the Cradle of Evolution in Africa to
820 Eurasia, Australia, and the Americas', *Journal of Virology,* 85 (6), 2964-74.
821 McMullen, A. R., et al. (2013), 'Molecular evolution of lineage 2 West Nile virus', *Journal of General*
822 *Virology,* 94, 318-25.
823 Mencattelli, G., et al. (2022), 'Epidemiology of West Nile virus in Africa: An underestimated threat',
824 *PLoS Negl Trop Dis,* 16 (1), e0010075.
825 Michel, Friederike, et al. (2018), 'West Nile Virus and Usutu Virus Monitoring of Wild Birds in
826 Germany', *International Journal of Environmental Research and Public Health,* 15 (1), 171.
827 Michel, Friederike, et al. (2019), 'Evidence for West Nile Virus and Usutu Virus Infections in Wild and
828 Resident Birds in Germany, 2017 and 2018', *Viruses,* 11 (7), 674.
829 Minh, B. Q., Nguyen, M. A., and von Haeseler, A. (2013), 'Ultrafast approximation for phylogenetic
830 bootstrap', *Molecular Biolology and Evolution,* 30 (5), 1188-95.
831 Minh, B. Q., et al. (2022), 'IQ-TREE version 2.2.0: Tutorials and Manual

832 Phylogenomic software by maximum likelihood', <http://www.iqtree.org/doc/iqtree-doc.pdf>,
833 accessed 15.09.2022.
834 Mishler, B. D. (2010), 'Species are not uniquely real biological entities', in F. J. Ayala and R. Arp (eds.),
835 *Contemporary Debates in Philosophy of Biology* (Malden (MA): Wiley-Blackwell), 110-22.
836 Muhire, B. M., Varsani, A., and Martin, D. P. (2014), 'SDT: A Virus Classification Tool Based on
837 Pairwise Sequence Alignment and Identity Calculation', *Plos One,* 9 (9).
838 Murgue, B., et al. (2001), 'West Nile outbreak in horses in Southern France, 2000: The return after 35
839 years', *Emerging Infectious Diseases,* 7 (4), 692-96.
840 Nguyen, L. T., et al. (2015), 'IQ-TREE: a fast and effective stochastic algorithm for estimating
841 maximum-likelihood phylogenies', *Molecular Biology and Evolution,* 32 (1), 268-74.
842 Pachler, K., et al. (2014), 'Putative new West Nile virus lineage in Uranotaenia unguiculata
843 mosquitoes, Austria, 2013', *Emerg Infect Dis,* 20 (12), 2119-22.
844 Paull, S. H., et al. (2017), 'Drought and immunity determine the intensity of West Nile virus epidemics
845 and climate change impacts', *Proceedings of the Royal Society B-Biological Sciences,* 284
846 (1848).
847 Perez-Ramirez, E., et al. (2017), 'Pathogenicity evaluation of twelve West Nile virus strains belonging
848 to four lineages from five continents in a mouse model: discrimination between three
849 pathogenicity categories', *J Gen Virol,* 98 (4), 662-70.
850 Pietsch, C., et al. (2020), 'Autochthonous West Nile virus infection outbreak in humans, Leipzig,
851 Germany, August to September 2020', *Eurosurveillance,* 25 (46).
852 Quick, J., et al. (2017), 'Multiplex PCR method for MinION and Illumina sequencing of Zika and other
853 virus genomes directly from clinical samples', *Nature Protocols,* 12 (6), 1261-76.
854 R Core Team (2022), 'R: A language and environment for statistical computing', <https://www.R-
855 project.org/>, accessed 12.09.2022.
856 Ragonnet-Cronin, M., et al. (2013), 'Automated analysis of phylogenetic clusters', *Bmc Bioinformatics,*
857 14 (1).
858 Rambaut, A., et al. (2016), 'Exploring the temporal structure of heterochronous sequences using
859 TempEst (formerly Path-O-Gen)', *Virus Evolution,* 2 (1).

Rambaut, A., et al. (2020), 'A dynamic nomenclature proposal for SARS-CoV-2 lineages to assist genomic epidemiology (vol 5, pg 1403, 2020)', *Nature Microbiology,* 5 (11), 1403–07.

Ravagnan, S., et al. (2015), 'First report outside Eastern Europe of West Nile virus lineage 2 related to the Volgograd 2007 strain, northeastern Italy, 2014', *Parasites & Vectors,* 8 (1).

Rizzoli, A., et al. (2015), 'The challenge of West Nile virus in Europe: knowledge gaps and research priorities', *Eurosurveillance,* 20 (20).

Robert-Koch-Institut (2020), 'Autochthone Infektionen mit dem West-Nil-Virus in Deutschland 2018 und 2019', *Epidemiologisches Bulletin*, 25, 3-10.

Ronca, S. E., Ruff, J. C., and Murray, K. O. (2021), 'A 20-year historical review of West Nile virus since its initial emergence in North America: Has West Nile virus become a neglected tropical disease?', *Plos Neglected Tropical Diseases,* 15 (5).

Rudolf, I., et al. (2014), 'West Nile virus lineage 2 isolated from Culex modestus mosquitoes in the Czech Republic, 2013: expansion of the European WNV endemic area to the North?', *Eurosurveillance,* 19 (31), 2-5.

Savage, H. M., et al. (1999), 'Entomologic and avian investigations of an epidemic of West Nile fever in Romania in 1996, with serologic and molecular characterization of a virus isolate from mosquitoes', *American Journal of Tropical Medicine and Hygiene,* 61 (4), 600-11.

Schneider, J., et al. (2021), 'Autochthonous West Nile virus infection in Germany: Increasing numbers and a rare encephalitis case in a kidney transplant recipient', *Transboundary and Emerging Disease*, 1-6.

Sedlak, K., et al. (2014), 'Surveillance of West Nile fever in horses in the Czech Republic from 2011 to 2013', *Epidemiologie Mikrobiologie Imunologie,* 63 (4), 307-11.

Sikkema, R. S., et al. (2020), 'Detection of West Nile virus in a common whitethroat (Curruca communis) and Culex mosquitoes in the Netherlands, 2020', *Eurosurveillance,* 25 (40).

Simmonds, P., et al. (2017), 'ICTV Virus Taxonomy Profile: Flaviviridae', *Journal of General Virology,* 98 (1), 2-3.

Smithburn, K. C., et al. (1940), 'A neurotropic virus isolated from the blood of a native of Uganda', *The American Journal of Tropical Medicine and Hygiene,* s1-20 (4), 471-92.

Suchard, M. A., et al. (2018), 'Bayesian phylogenetic and phylodynamic data integration using BEAST 1.10', *Virus Evolution,* 4 (1), vey016.

Tsai, T. F., et al. (1998), 'West Nile encephalitis epidemic in southeastern Romania', *Lancet,* 352 (9130), 767-71.

Ulbert, S. (2019), 'West Nile virus vaccines - current situation and future directions', *Human Vaccines & Immunotherapeutics,* 15 (10), 2337-42.

Vlckova, J., et al. (2015), 'West Nile virus transmission risk in the Czech Republic', *Epidemiologie Mikrobiologie Imunologie,* 64 (2), 80-86.

Wylezich, C., et al. (2018), 'A Versatile Sample Processing Workflow for Metagenomic Pathogen Detection', *Scientific Reports,* 8 (1), 13108.

Wylezich, C., et al. (2021), 'Next-generation diagnostics: virus capture facilitates a sensitive viral diagnosis for epizootic and zoonotic pathogens including SARS-CoV-2', *Microbiome,* 9 (1), 51.

Zehender, G., et al. (2017), 'Reconstructing the recent West Nile virus lineage 2 epidemic in Europe and Italy using discrete and continuous phylogeography', *Plos One,* 12 (7).

Ziegler, U., et al. (2019), 'West Nile virus epizootic in Germany, 2018', *Elsevier,* 162, 39-43.

Ziegler, U., et al. (2020), 'West Nile Virus Epidemic in Germany Triggered by Epizootic Emergence, 2019', *Viruses,* 12 (4).

Ziegler, U., et al. (2022), 'Spread of West Nile Virus and Usutu Virus in the German Bird Population, 2019-2020', *Microorganisms,* 10 (4).

908 **Table 1** Overview of WNV cases analyzed in this study. Sample numbers are used in Figures 4 and 7.

Sample no.	Sample ID	Library ID	Sequence accession	Common English name	Scientific name	Collection date	Federal state[1]
1	**167/20**	**lib04566**		Blue tit	*Cyanistes caeruleus*	07.07.2020	BE
2	**174/20**	**lib04567**		Snowy owl	*Bubo scandiacus*	12.07.2020	TH
3	**192/20**	**lib04568**		Snowy owl	*Bubo scandiacus*	15.08.2020	TH
4	**193/20**	**lib04569**		Northern goshawk	*Accipiter gentilis*	30.07.2020	SN
5	**200/20**	**lib04570**		Bohemian waxwing	*Bombycilla garrulus*	11.08.2020	BB
6	**203/20**	**lib04571**		Little owl	*Athene noctua*	18.08.2020	BB
7	**206/20**	**lib04572**		Northern goshawk	*Accipiter gentilis*	08.08.2020	BE
8	**214/20**	**lib04573**		Unspecified flamingo	*Phoenicopterus sp.*	19.08.2020	TH
9	**218/20**	**lib04574**		Unspecified flamingo	*Phoenicopterus sp.*	18.08.2020	ST
10	**339/20**	**lib04575**		Chilean flamingo	*Phoenicopterus chilensis*	25.08.2020	BE
11	**252/20**	**lib04576**		Eurasian jay	*Garrulus glandarius*	Aug. /Sept.2020	TH
12	**283/20**	**lib04577**		Snowy owl	*Bubo scandiacus*	02.09.2020	ST
13	**207/20**	**lib04717**		Northern goshawk	*Accipiter gentilis*	09.08.2020	BE
14	**208/20**	**lib04718**		Northern goshawk	*Accipiter gentilis*	14.08.2020	BB
15	**211/20**	**lib04719**		Blue tit	*Cyanistes caeruleus*	August 2020	BE
16	**194/20**	**lib04720**		Blue tit	*Cyanistes caeruleus*	August 2020	SN
17	**268/20 Nr. 1**	**lib04721**		Little owl	*Athene noctua*	September 2020	BB
18	**311/20**	**lib04722**		Northern goshawk	*Accipiter gentilis*	Sept./Okt. 2020	BE
19	**314/20**	**lib04723**		Northern goshawk	*Accipiter gentilis*	Sept./Okt. 2020	BE
20	**315/20**	**lib04724**		Northern goshawk	*Accipiter gentilis*	Sept./Okt. 2020	BE
21	**224/20**	**lib04725**		Blue tit	*Cyanistes caeruleus*	August 2020	BE
22	**282/20**	**lib04726**		Snowy owl	*Bubo scandiacus*	02.09.2020	ST
23	**281/20**	**lib04727**		Unspecified flamingo	*Phoenicopterus sp.*	September 2020	ST
24	**340/20**	**lib04728**		American flamingo	*Phoenicopterus ruber*	22.08.2020	BE
25	**196/20**	**lib04729**		Unspecified buzzard	*Buteo sp.*	August 2020	SN
26	**258/20**	**lib04730**		Great tit	*Parus major*	Aug. /Sept.2020	SN
27	**242/20**	**lib04731**		Northern goshawk	*Accipiter gentilis*	August 2020	BE
28	**245/20**	**lib04732**		Unspecified flamingo	*Phoenicopterus sp.*	August 2020	BE
29	**260/20**	**lib04733**		Domestic canary	*Serinus canaria forma domestica*	September 2020	ST

Sample no.	Sample ID	Library ID	Sequence accession	Common English name	Scientific name	Collection date	Federal state[1]
30	**261/20**	**lib04734**		Chilean flamingo	*Phoenicopterus chilensis*	September 2020	SN
31	**264/20**	**lib04735**		Unspecified sparrow	*Passer sp.*	September 2020	SN
32	**228/20**	**lib04736**		Horse	*Equus caballus*	02.09.2020	SN
33	**173/20**	**lib04737**		Alpine chough	*Pyrrhocorax graculus*	12.07.2020	ST
34	**216/20**	**lib04738**		Blue tit	*Cyanistes caeruleus*	August 2020	TH
35	**199/20**	**lib04739**		Northern goshawk	*Accipiter gentilis*	13.06.2020	BE
36	**205/20**	**lib04740**		Northern goshawk	*Accipiter gentilis*	13.08.2020	BE
37	**210/20**	**lib04741**		Northern goshawk	*Accipiter gentilis*	01.08.2020	BE
38	**238/20**	**lib04742**		Northern goshawk	*Accipiter gentilis*	31.08.2020	BE
39	**241/20**	**lib04743**		Northern goshawk	*Accipiter gentilis*	23.08.2020	BE
40	**244/20**	**lib04744**		Hooded crow	*Corvus corone cornix*	18.08.2020	BE
41	**219/20**	**lib04745**		Chilean flamingo	*Phoenicopterus chilensis*	26.08.2020	ST
42	**284/20**	**lib04746**		Swift parrot	*Lathamus discolor*	21.09.2020	ST
43	**286/20**	**lib04747**		Horse	*Equus caballus*	29.09.2020	ST
44	**246/20**	**lib04757**		Golden eagle	*Aquila chrysaetos*	(09.09.2020) survived	BB
45	**201/20**	**na[2]**		European greenfinch	*Carduelis chloris*	07.07.2020	BB
46	**60/21**	**lib04758**		Blue tit	*Cyanistes caeruleus*	2020	TH
C4	**115/19**	**lib04565**		Chinese merganser	*Mergus squamatus*	08.08.2019	BE
C5	**127/18**	**lib04748**		Horse	*Equus caballus*	11.09.2018	BB

[1] Abbreviations for federal states: BE, Berlin; BB, Brandenburg; SN, Saxony; ST, Saxony Anhalt; TH, Thuringia

[2] WNV-specific multiplex PCR was unsuccessful due to low amount of WNV-RNA in the sample (Cq 36).

911 **Table 2** Overview of terms commonly used for the designation of virus sequences into groups below the species rank.

		Current common use in the WNV research community			Proposed use	
Term	**General definition**	**Definition**	**Example lineage 1**	**Example lineage 2**	**Level below species/term**	**Example designation**
Lineage	Rank-independent term for the relationships between ancestors and descendants through time (diachronic). Typically, a higher resolution classification compared to clade. (Campbell et al. 2022; Cellinese et al. 2012; Rambaut et al. 2020)	Broadest monophyletic group below the WNV species rank. There are 9 proposed WNV lineages. (Fall et al. 2017)	Lineage 1; Lineage 1a	Lineage 2	1 / Lineage	Lineage 1; Lineage 2
Clade	Rank-independent term for a monophyletic group on a phylogenetic tree. Mishler (2010), describe it as "a monophyletic group is all and only the descendants of common ancestors" (synchronic). (Campbell et al. 2022; Cellinese et al. 2012; Rambaut et al. 2020)	Smaller monophyletic group within the lineage. Typically denoted with letters. Example, 1a - 1c and 2a-2d (May et al. 2011; McMullen et al. 2013). In Lineage 2, this level also describes a monophyletic group sharing similar geographic range. (Ziegler et al. 2020)	Clade 1a	Clade 2d; Central/ Southern European clade	2 / Clade	Clade 1.1; Clade 2.5
Subclade	A smaller monophyletic group within a larger clade (Campbell et al. 2022)	Smaller monophyletic group within the clade. More often used in Lineage 2. In Lineage 2, these are also used to describe sequences from a monophyletic branch sharing geographic range. (Barzon et al. 2015; Ziegler et al. 2020)	Not commonly used in Lineage 1	Central/Southern European subclade; subclade: "Eastern German clade"	3 / Subclade	Subclade 1.1.4; Subclade 2.5.1

		Current common use in the WNV research community			Proposed use	
Term	**General definition**	**Definition**	**Example lineage 1**	**Example lineage 2**	**Level below species/term**	**Example designation**
Cluster	Closely related sequences sharing a certain threshold of nucleotide or amino acid identities, characteristics, or provides to define cluster of disease transmission. (Han et al. 2019)	Smaller monophyletic group within the clade in Lineage 1, sharing a single ancestor and or a fixed unique non-synonymous mutation (May et al). Smaller monophyletic group within the clade or subclade in Lineage 2. (Barzon et al. 2015)	Cluster 1	Italian Lombardy cluster	4 / Cluster	Cluster 1.1.4.1 or Subclade 1.1.4 cluster 1; Cluster 2.5.1.1 or Subclade 2.5.1 cluster 1
Subtype	A subset of a species based on a certain characteristic	Below Cluster level, to designate WNV cluster 2 based on geographic location. (May et al. 2011)	Mediterranean subtype (cluster 2)	not commonly used in Lineage 2	5 / Subcluster (designated by 5th decimal place)	Subcluster 1.1.4.1.6; Subluster 2.5.1.1.5
Genotype	monophyletic cluster of sequences with high statistical support (Goya et al. 2020)	Used to describe different sequences of WNV lineage 1 cluster 4 detected in America, which shared fixed nonsynonymous mutation. Sub-type was not described in cluster 4 (Mann et al. 2013).	NY99 genotype (cluster 4)	not commonly used in Lineage 2	6 / Subcluster (designated by a letter as suffix)	Subcluster 1.1.4.1.6a; Subcluster 2.5.1.1.5a

912

913

914 **Table 3** Summary of avian species infected with WNV in 2020 in Germany

Order	Common English Name	Scientific Name	Housing	Number	Affected Federal State[1]
Accipitriformes	Unspecified buzzard	*Buteo sp.*	wild	1	SN
	Northern goshawk	*Accipiter gentilis*	wild/captive	17	BE, BB, SN
	Golden eagle	*Aquila chrysaetos*	captive	1	BB
Charadriiformes	Black-tailed gull	*Larus crassirostris*	captive	1	BE
Passeriformes	Alpine chough	*Pyrrhocorax graculus*	captive	1	ST
	Blue tit	*Parus caeruleus*	wild	8	BE, SN, TH
	Eurasian jay	*Garrulus glandarius*	wild	1	TH
	European greenfinch	*Carduelis chloris*	wild	1	BB
	Domestic canary	*Serinus canaria forma domestica*	captive	1	ST
	Great tit	*Parus major*	wild	1	SN
	Hooded crow	*Corvus corone cornix*	wild	2	BE
	Bohemian waxwing	*Bombycilla garrulus*	captive	1	BB
	Unspecified sparrow	*Passer sp.*	wild	1	SN
Phoenicopteriformes	Chilean flamingo	*Phoenicopterus chilensis*	captive	6	BE, ST, SN
	American flamingo	*Phoenicopterus ruber*	captive	1	BE
	Unspecified flamingo	*Phoenicopterus sp.*	captive	8	BE, ST, TH
Psittaciformes	Swift parrot	*Lathamus discolor*	captive	2	ST
Strigiformes	Snowy owl	*Bubo scandiacus*	captive	4	ST, TH
	Little owl	*Athene noctua*	captive	5	BB
	Barn owl	*Tyto alba*	wild	1	BB
	Eurasian eagle-owl	*Bubo bubo*	captive	1	ST

915 [1] Abbreviations for federal states: BE, Berlin; BB, Brandenburg; SN, Saxony; ST, Saxony Anhalt; TH, Thuringia

916 **Figure legends**

917

918 **Figure 1** Graphical representation of the proposed hierarchy and the corresponding group labels.
919 The levels of the proposed are ordered top to bottom; the corresponding group label is organized left
920 to right. Note that the subcluster can either have the number only or the number combined with a
921 letter.

922

923 **Figure 2** Comparison of APC groupings of test dataset TD03 with previously defined groupings and
924 phylogenetic reconstruction.
925 The representation of the objective APC grouping includes the addressed hierarchical levels, starting
926 with lineage, decreasing from left to right down to the subclade. The vertical lines mark the final level
927 down to which the grouping could be done (limited either by the minimum group size applied for the
928 input of subgrouping or by the hierarchical level that was the last to be shown). Horizontal lines
929 separate the individual groups. Each group is labelled at the right-hand side of the graph. Dashed
930 vertical lines with arrows connect areas of the graph together forming one common group
931 interspersed by other group(s). The horizontal grey rectangle labelled “X” marks a sequence that was
932 not considered for APC/AHC grouping due to its high number of ambiguities (>=10). For comparison,
933 the groupings that were previously published by Fall et al. (2017) and May et al. (2011) are included.
934 Here, a filled circle represents a singleton sequence making up the respective group as labelled and
935 two filled circles connected by a vertical line represent a larger group. White rectangles mark
936 sequences included in the tree but not part of the cited analyses. The maximum likelihood (ML)
937 phylogenetic analysis of sequences from TD03 was done with the best fitting model GTR+I+G and
938 100,000 ultrafast bootstraps. Few large branches consisting of sequences from almost the same
939 geographic regions are collapsed into triangles. The nodes are labelled with ultrafast bootstrap values.

940

941 **Figure 3** Comparison of APC groupings of WNV lineage 2 (WL2) sequences with previously defined
942 groupings and phylogenetic reconstruction.

943 The representation of the objective APC grouping includes the addressed hierarchical levels, starting
944 with lineage (not calculated here but WNV lineage 2 sequences included according to published
945 references), decreasing from left to right down to the cluster. The vertical lines mark the final level
946 down to which the grouping could be done (limited either by the minimum group size applied for the
947 input of subgrouping or by the hierarchical level that was the last to be shown). Horizontal lines
948 separate the individual groups. Each group is labelled at the right-hand side of the graph. Dashed
949 vertical lines with arrows connect areas of the graph together forming one common group
950 interspersed by other group(s). The horizontal grey rectangle labelled "X" marks a sequence that was
951 not considered for APC/AHC grouping due to its high number of ambiguities (>=10). For comparison,
952 the groupings that were previously published by Chaintoutis et al. (2019), McMullen et al. (2013),
953 Ravagnan et al. (2015), Zehender et al. (2017) and Ziegler et al. (2020) are included. Here, a filled circle
954 represents a singleton sequence making up the respective group as labelled and two filled circles
955 connected by a vertical line represent a larger group. White rectangles mark sequences included in the
956 tree but not part of the cited analyses. The maximum likelihood (ML) phylogenetic analysis of
957 sequences from WL2 was done with the best fitting model GTR+I+G and 100,000 ultrafast bootstraps.
958 Few large branches consisting of sequences from almost the same geographic regions are collapsed
959 into triangles. The nodes are labelled with ultrafast bootstrap values.
960
961 **Figure 4** Bayesian maximum clade credibility (MCC) tree representing time scaled phylogeny of
962 European WNV subclade 2.5.3 complete coding sequences together with objective APC groups.
963 WNV sequences acquired in this study are highlighted yellow. All other WNV sequences were retrieved
964 from GenBank and are listed in Table S3. The colored branches of MCC trees represent the most
965 probable geographic location of their descendants (see legend "locations"). Bayesian posterior
966 probabilities are indicated at each node. Time (in years) is indicated as x-axis below the MCC tree. The
967 time for the most recent common ancestor (MRCA), time intervals defined by the 95% highest
968 posterior density (95% HPD), and posterior probabilities (pp) are shown in the following nodes that
969 consist of the following WNV sequences: (i) LR743448 and MW036634, (ii) cluster 2.5.3.2 sequences,

and (iii) subcluster 2.5.3.4.3c sequences. The representation of the objective APC grouping includes the addressed hierarchical levels, starting with cluster decreasing from left to right down to the subcluster. The vertical lines mark the final level down to which the grouping could be done (limited either by the minimum group size applied for the input of subgrouping or by the hierarchical level that was the last to be shown). Horizontal lines separate the individual groups. Each group is labelled at the right-hand side of the graph. Dashed vertical lines with arrows connect areas of the graph together forming one common group interspersed by other group(s).

Figure 5 Notifiable WNV-cases of birds and horses in Germany from 2018 –20.
The number of cases were summed up per federal state and year. Notifiable cases in horses and birds were represented by blue and red bars, respectively. Abbreviations of federal states in Germany: BB – Brandenburg, BE – Berlin, BY – Bavaria, HH – Hamburg, NI – Lower Saxony, MV - Mecklenburg Western Pomerania, SN – Saxony, ST – Saxony-Anhalt, and TH – Thuringia.

Figure 6 Geographic distribution of WNV cases in Germany from 2018-20 per host and (sub)clusters.
Labelling according to the legend in the graph. WNV-positive cases confirmed by the National Reference Laboratory without complete coding sequences are depicted in grey (labelled "undetermined" in the legend).

Figure 7 Summarized geographic distribution of WNV cases in Germany from 2018 –20.
Labelling according to the legend in the graph. WNV-positive cases confirmed by the National Reference Laboratory without complete coding sequences are depicted in grey (labelled "undetermined" in the legend). Districts colored gray indicate areas with (additional) WNV-positive cases from WNV seasons 2018-19 without a complete coding sequence. Areas with high WNV activity in 2020 are shown in enlarged and separated maps, (B) Berlin, (C) Saxony, Saxony-Anhalt and Thuringia. New WNV cases from this study are indicated with numbers as described in Table 1.

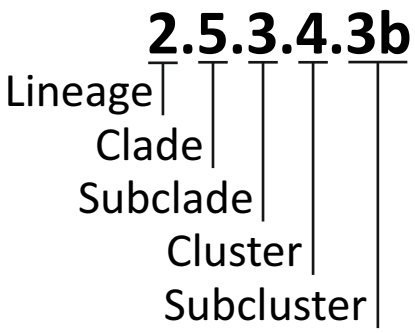

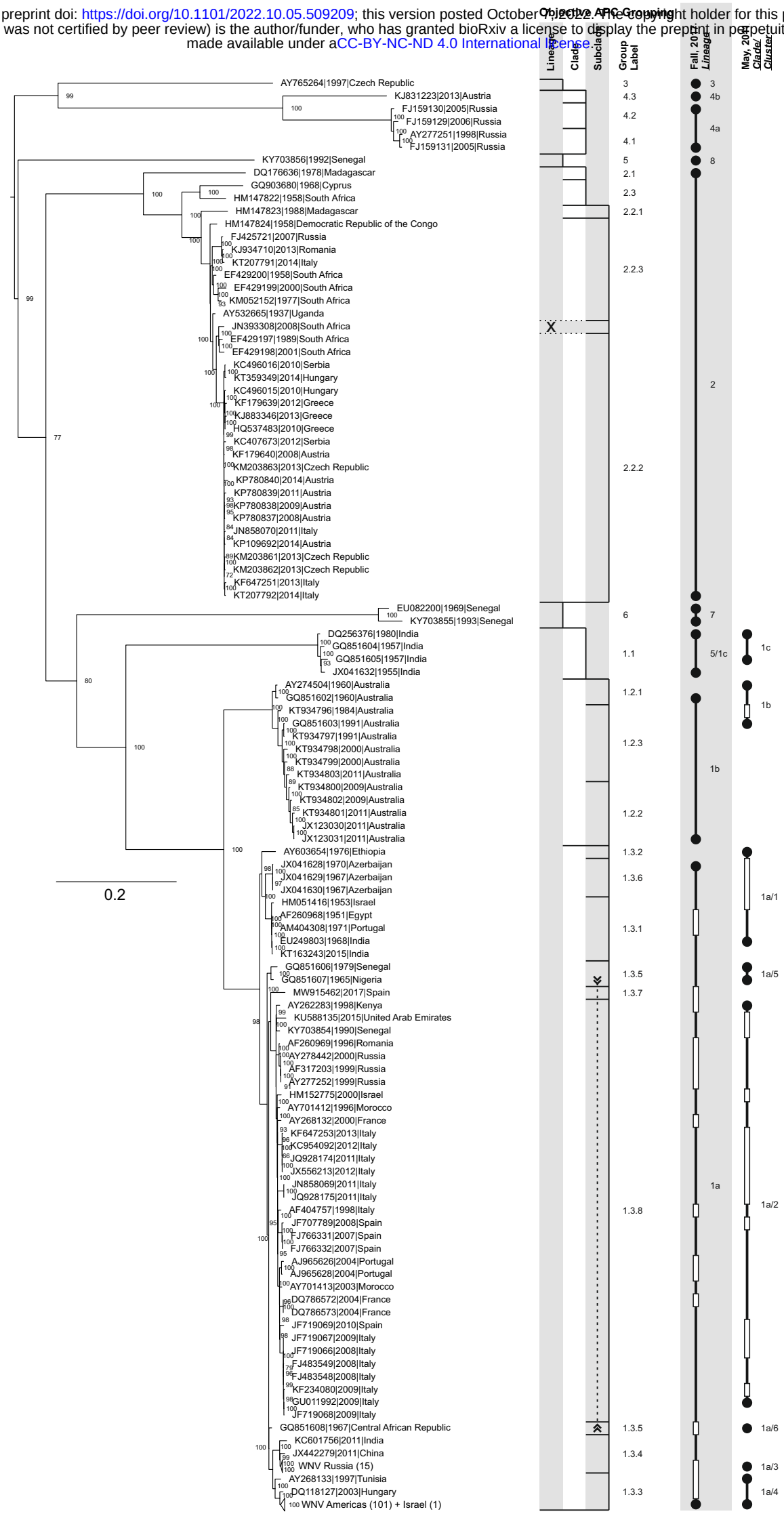

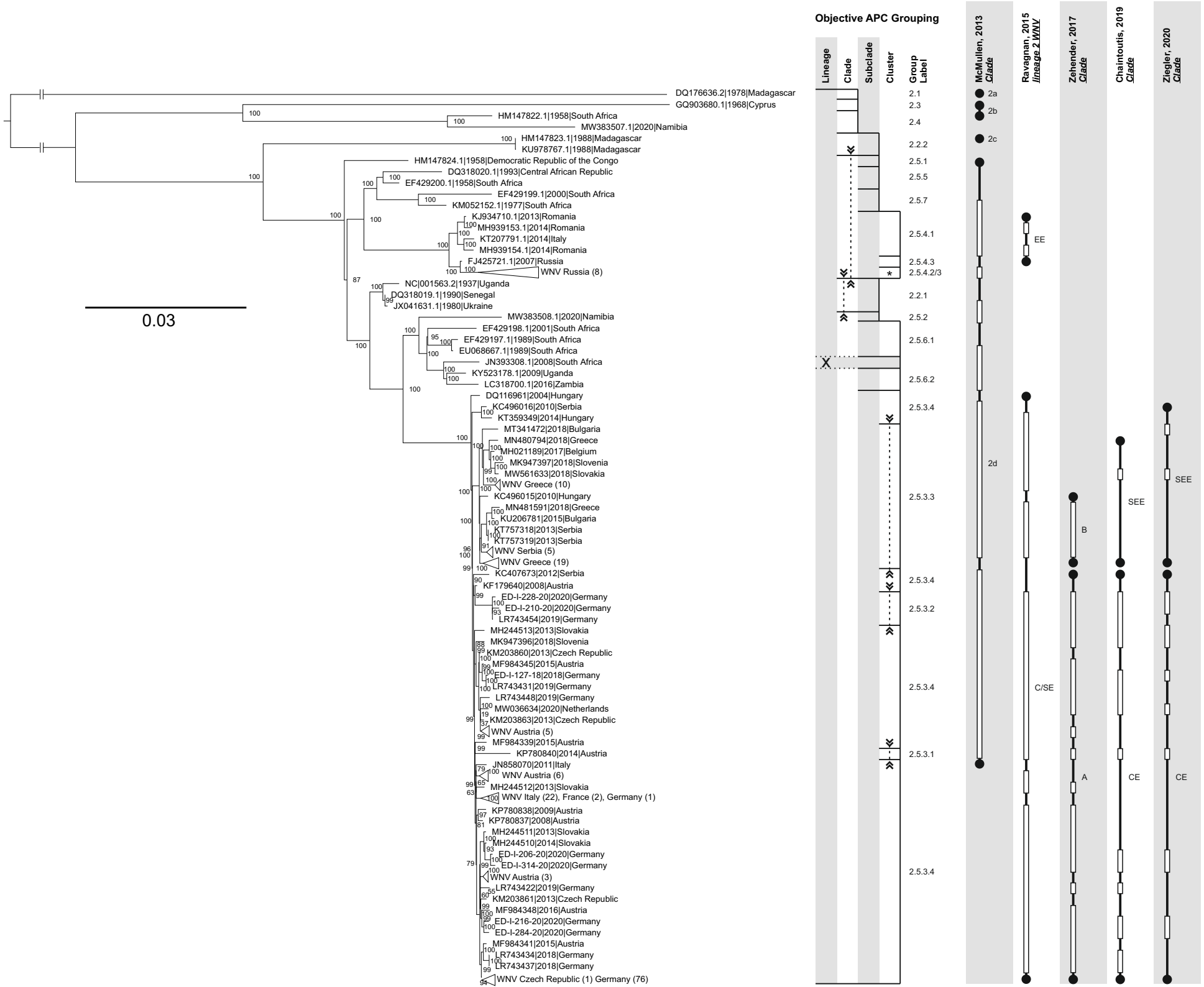
DQ176636.2|1978|Madagascar
GQ903680.1|1968|Cyprus
HM147822.1|1958|South Africa
MW383507.1|2020|Namibia
HM147823.1|1988|Madagascar
KU978767.1|1988|Madagascar
HM147824.1|1958|Democratic Republic of the Congo
DQ318020.1|1993|Central African Republic
EF429200.1|1958|South Africa
EF429199.1|2000|South Africa
KM052152.1|1977|South Africa
KJ934710.1|2013|Romania
MH939153.1|2014|Romania
KT207791.1|2014|Italy
MH939154.1|2014|Romania
FJ425721.1|2007|Russia
WNV Russia (8)
NC|001563.2|1937|Uganda
DQ318019.1|1990|Senegal
JX041631.1|1980|Ukraine
0.03
MW383508.1|2020|Namibia
EF429198.1|2001|South Africa
EF429197.1|1989|South Africa
EU068667.1|1989|South Africa
JN393308.1|2008|South Africa
KY523178.1|2009|Uganda
LC318700.1|2016|Zambia
DQ116961|2004|Hungary
KC496016|2010|Serbia
KT359349|2014|Hungary
MT341472|2018|Bulgaria
MN480794|2018|Greece
MH021189|2017|Belgium
MK947397|2018|Slovenia
MW561633|2018|Slovakia
WNV Greece (10)
KC496015|2010|Hungary
MN481591|2018|Greece
KU206781|2015|Bulgaria
KT757318|2013|Serbia
KT757319|2013|Serbia
WNV Serbia (5)
WNV Greece (19)
KC407673|2012|Serbia
KF179640|2008|Austria
ED-I-228-20|2020|Germany
ED-I-210-20|2020|Germany
LR743454|2019|Germany
MH244513|2013|Slovakia
MK947396|2018|Slovenia
KM203860|2013|Czech Republic
MF984345|2015|Austria
ED-I-127-18|2018|Germany
LR743431|2019|Germany
LR743448|2019|Germany
MW036634|2020|Netherlands
KM203863|2013|Czech Republic
WNV Austria (5)
MF984339|2015|Austria
KP780840|2014|Austria
JN858070|2011|Italy
WNV Austria (6)
MH244512|2013|Slovakia
WNV Italy (22), France (2), Germany (1)
KP780838|2009|Austria
KP780837|2008|Austria
MH244511|2013|Slovakia
MH244510|2014|Slovakia
ED-I-206-20|2020|Germany
ED-I-314-20|2020|Germany
WNV Austria (3)
LR743422|2019|Germany
KM203861|2013|Czech Republic
MF984348|2016|Austria
ED-I-216-20|2020|Germany
ED-I-284-20|2020|Germany
MF984341|2015|Austria
LR743434|2018|Germany
LR743437|2018|Germany
WNV Czech Republic (1) Germany (76)
Objective APC Grouping
Lineage
Clade
Subclade
Cluster
Group Label
2.1
2.3
2.4
2.2.2
2.5.1
2.5.5
2.5.7
2.5.4.1
2.5.4.3
2.5.4.2/3
2.2.1
2.5.2
2.5.6.1
X
2.5.6.2
2.5.3.4
2.5.3.3
2.5.3.4
2.5.3.2
2.5.3.4
2.5.3.1
2.5.3.4
McMullen, 2013 Clade
2a
2b
2c
2d
Ravagnan, 2015 lineage 2 WNV
EE
C/SE
Zehender, 2017 Clade
B
A
Chaintoutis, 2019 Clade
SEE
CE
Ziegler, 2020 Clade
SEE
CE

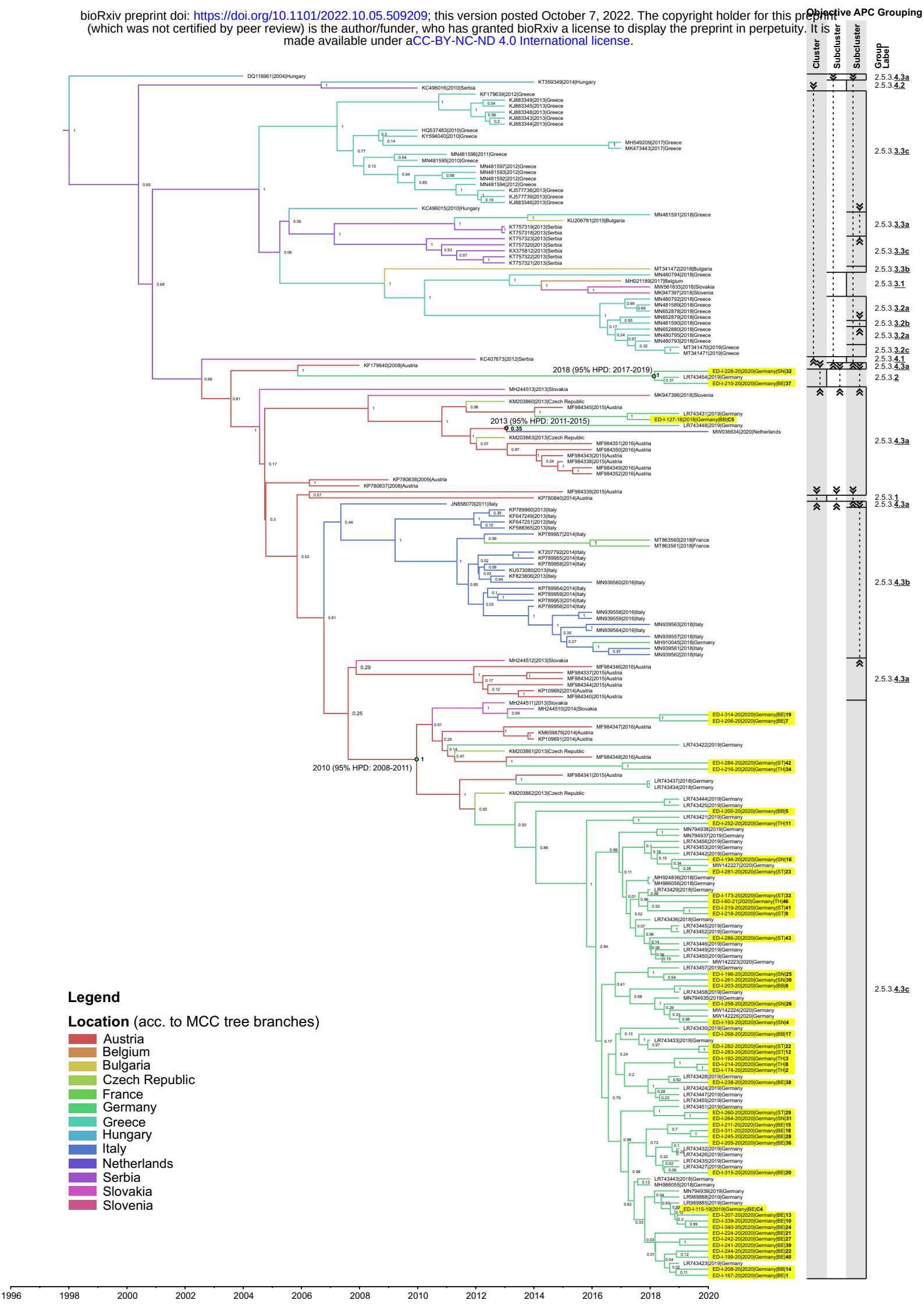

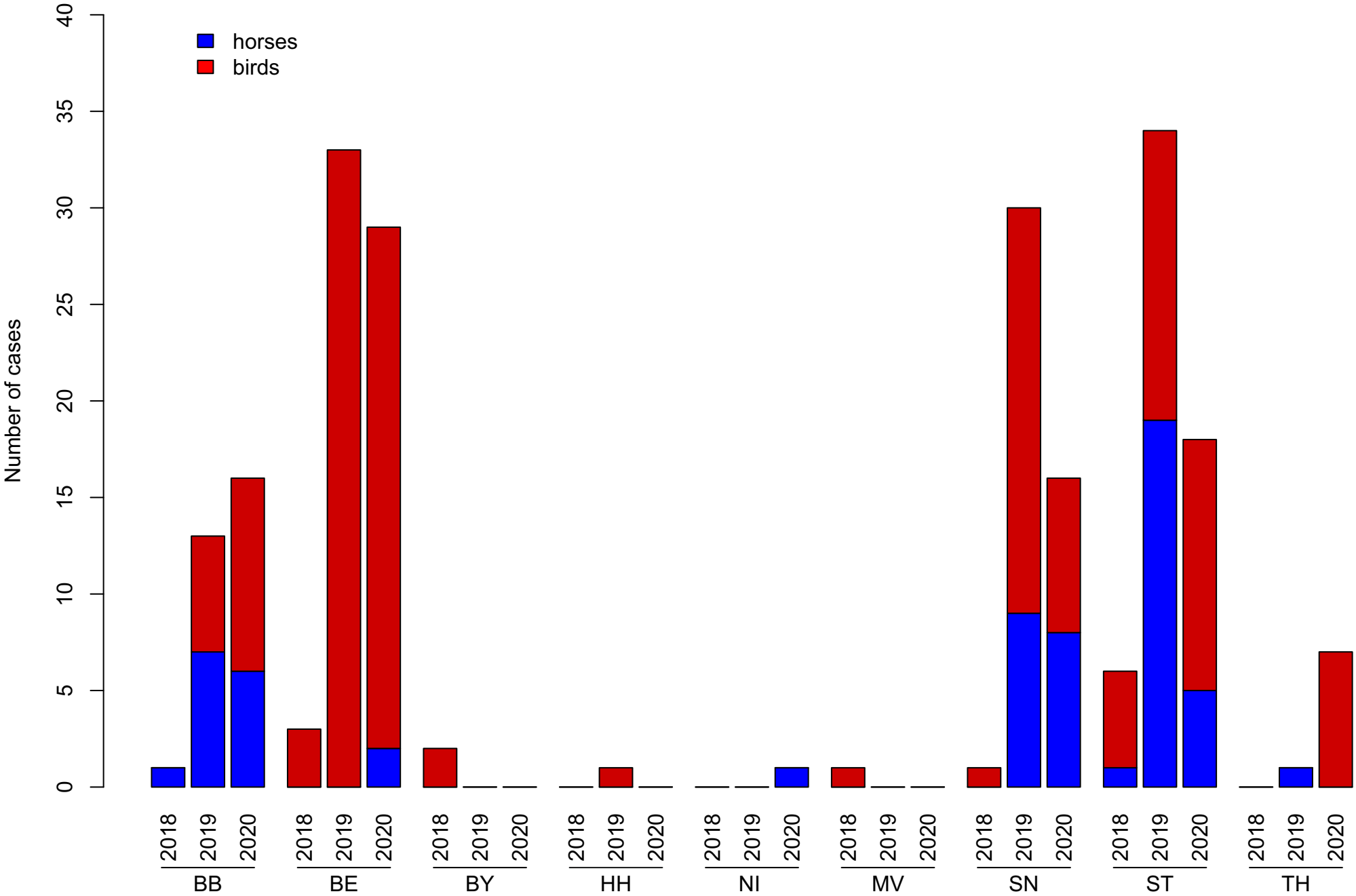
horses
birds
Number of cases
0
5
10
15
20
25
30
35
40
2018
2019
2020
BB
BE
BY
HH
NI
MV
SN
ST
TH

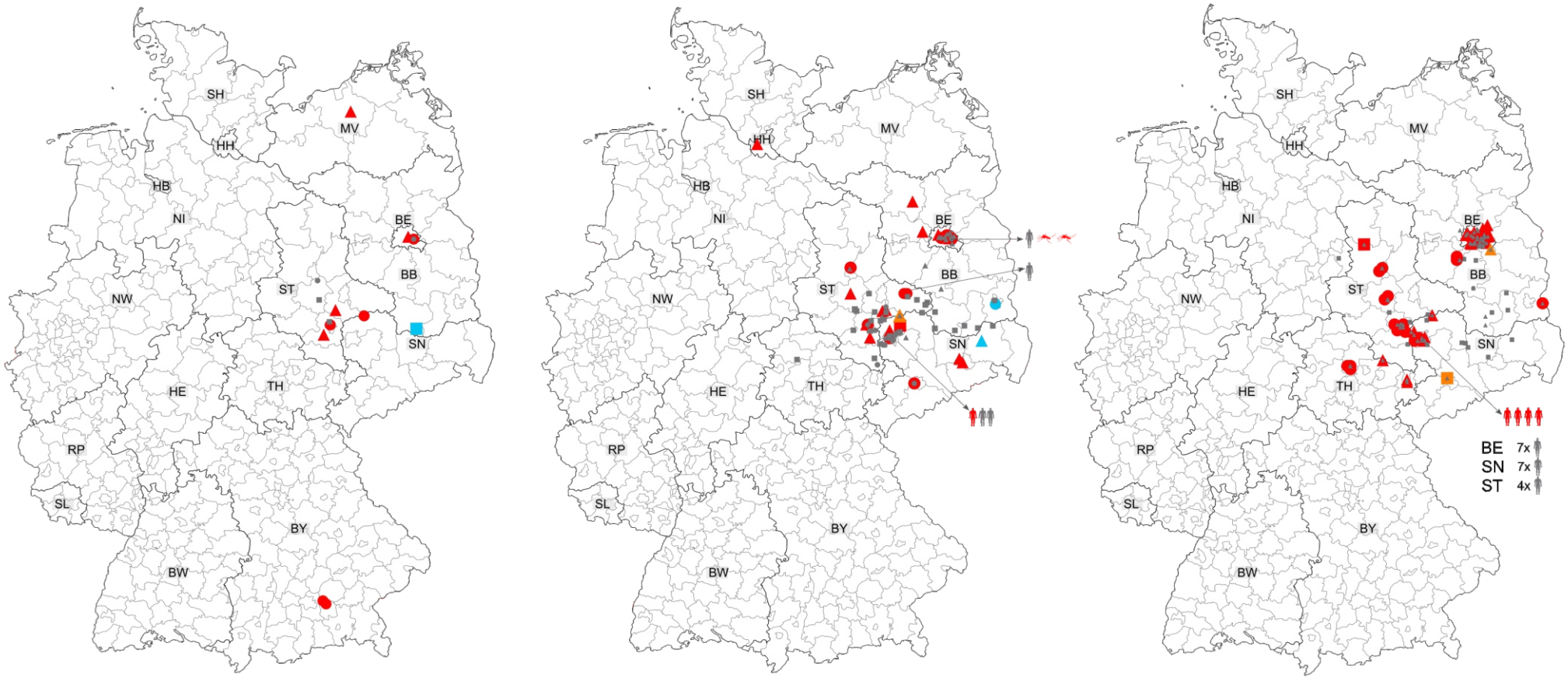

Legend

Federal States

BB – Brandenburg	NI – Lower Saxony
BE – Berlin	NW – North Rhine-Westphalia
BW – Baden-Württemberg	RP – Rhineland-Palatinate
BY – Bavaria	SH – Schleswig-Holstein
HB – Bremen	SL – Saarland
HE – Hesse	SN – Saxony
HH – Hamburg	ST – Saxony-Anhalt
MV – Mecklenburg-West Pomerania	TH – Thuringia

WNV cases

Host (shape)

- Captive bird
- Wild bird
- Horse
- Mosquito
- Human

Clusters and subclusters (fill color)

- 2.5.3.2
- 2.5.3.4.3a
- 2.5.3.4.3c
- undetermined

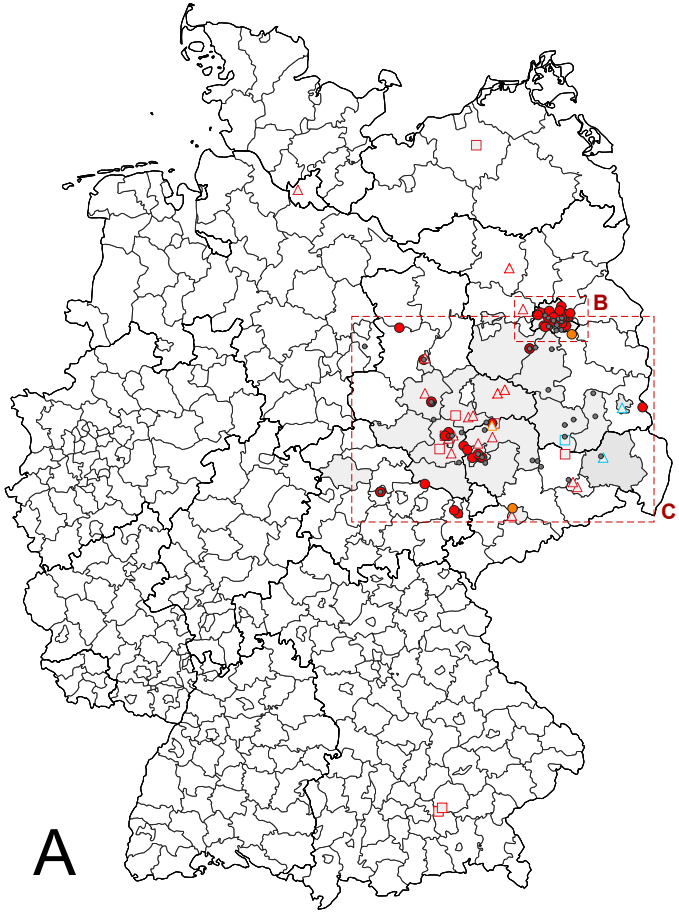

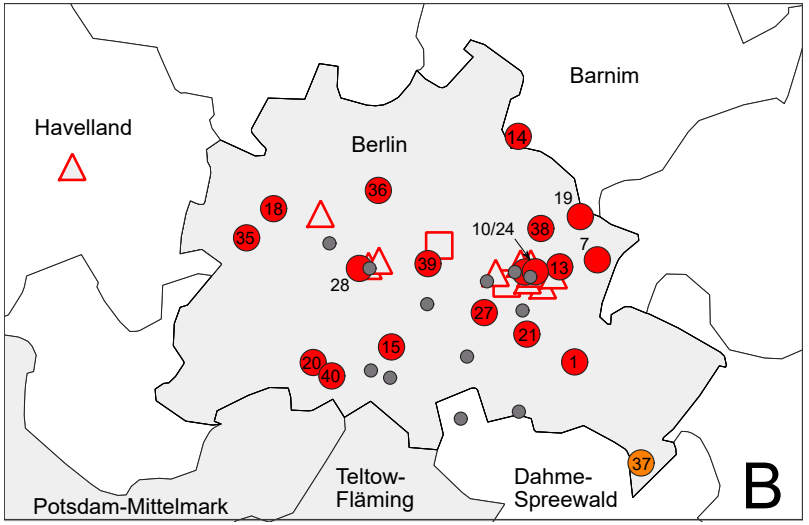

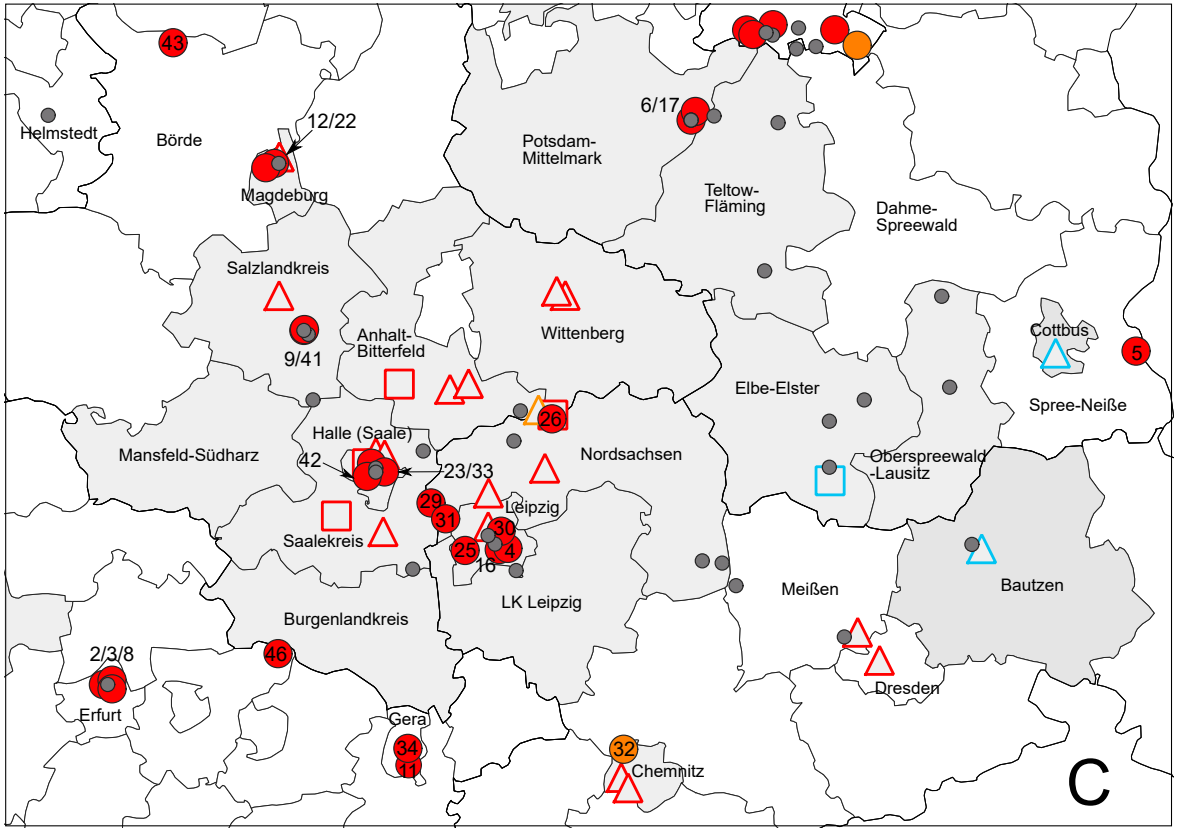

Legend

WNV cases in the years

Grouping	2018	2019	2020
2.5.3.2	ND	△	●
2.5.3.4.3a	□	△	ND
2.5.3.4.3c	□	△	●
Undetermined			●

Supplementary material for

"An advanced sequence clustering and designation workflow reveals the enzootic maintenance of a dominant West Nile virus subclade in Germany"

Pauline Dianne Santos[1,†], Anne Günther[1,†], Markus Keller[2], Timo Homeier-Bachmann[3], Martin H. Groschup[2,4], Martin Beer[1], Dirk Höper[1,†], Ute Ziegler[2,4, †,*]

Contents

R-Code

```
### AP-Clustering of genome sequences based on an identity-matrix


## load necessary R-packages

library(apcluster)

library(writexl)


## prepare workspace

rm(list = ls())  # clean up workspace to prevent from interference between calculation and pre-existing data


## settings; when multiple values are provided, all possible combinations are tested

minStepNumbers <- c(1000, 2000, 5000, 10000)  # the minimum number of steps to divide the input preference range for plateau calculations

stepFactor <- 10  # currently not used; Factor to calculate th allowed maximum step number from the used minStepNumbers

windowProportions <- c(0.01, 0.005, 0.0025, 0.001, 0.0001)  # the fraction of the complete steps (see above) the partial dataset used for the APC should have

minPlateauWindows <- 3  # the allowed minimum the actual window may have (values < 3 do not make sense)

groupSizes <- c(5, 7, 10)  # the minimum number of sequences of a subgroup to use as input for a further subgrouping

maxGroupDepth <- 5   # number of hierarchy levels to calculate with 1=Lineage/2=Clade/3=Subclade/4=Cluster/5=Subcluster


## load and prepare input data

setwd("M:/R-work/PS_wnv_apc/testWL2/")  # choose the folder to read the input from and to save the output

dateipfad <- "M:/R-work/PS_wnv_apc/testWL2/WL2_R01_cleaned.csv"  # choose the input file

sequenceIdentityMatrix <- read.csv(dateipfad, row.names = 1)  # read in the matrix of sequence identities



if(identical(colnames(sequenceIdentityMatrix), rownames(sequenceIdentityMatrix))) {    # check whether or not the dimnames are identical, if not do not calculate because it might generate invalid results

  dissimilarityMatrix <- -1*((1-as.matrix(sequenceIdentityMatrix))^2)  # convert the sequence identity matrix into a matrix of dissimilarities as this is the input for affinity propagation clustering

  for(aktStepNumber in minStepNumbers) {  # iterate the calculations over all preset numbers of steps over the input preference range

    for(winProp in windowProportions) {  # iterate the calculations over all preset proportions for plateau definition

      for(aktGroupSize in groupSizes) {  # iterate the calculations over all preset minimum group sizes
```

```
for(aktPlateauWindow in minPlateauWindows) {

  dateien <- list.files()  # read in a list of files currently present in your target folder

  ## prepare necessary objects to accomodate results

  paramCollection <- data.frame(level = NA, group = NA, inputGroupSize = NA, usedStepWidth =
NA, setIterations = NA,
                                usedIterations = NA, minPrefRange = NA, maxPrefRange = NA,
terminatingInPref = NA,
                                defaultStepNumber = NA, lastStable = NA, longest = NA, defaultAPC = NA,
                                cutCrit = NA, usedWindowSize = NA)  # set up a data.frame to collect all
relevant parameters used in the current iteration

  allResults <- vector("list", 4)  # set up a list to collect all clustering results from the current
iteration

  names(allResults) <-  c("group", "defaultAPresult", "cutreeResult", "aggExResult")  # name the
elements of the list


  ## calculate settings adjusted according to above input

  maxStepNumber <- aktStepNumber * stepFactor  # currently not used; calculate the
maximum allowed step number

  initSteps <- (aktStepNumber + maxStepNumber) / 2  # currently not used; calculate the initial
number of steps to start with

  plateauWindow <- floor(aktStepNumber * winProp)    # set the window size to fit the actual
step number and interrogate always the same portion of the overall range

  if(plateauWindow < aktPlateauWindow) plateauWindow <- aktPlateauWindow  ## in case the
combined settings result in a window smaller than the minimum allowed window size, adjust the
setting to the allowed minimum


  ## prepare filenames to save results

  datensatz <- sub("\\.[[:alpha:]]{1,}$", "", basename(dateipfad))  # extract the name of the
dataset from the filepath

  filename <- paste(datensatz, ".test.Affiliations-minSteps_", aktStepNumber, "-window_",
plateauWindow,
                    "-minMembers_", aktGroupSize, "-maxGroupDepth_", maxGroupDepth, ".xlsx", sep
= "")  # construct filename containing the distinguishing parameters


  if(is.element(filename, dateien) == FALSE) {  # check whether the calculation using the
recent parameter combination was already initiated; only if not, continue calculating, otherwise
skip to the next combination

    write_xlsx(data.frame("Analysis in progress"), filename, col_names = FALSE)  # write a file
into the current folder to mark the parameter combination in progress

    print(paste("Analysis in progress: ", filename, sep = ""))  # output user information


    seqSubset <- colnames(dissimilarityMatrix)    # define the initial set of sequences, i.e. use
all sequences of the dataset

    affiliations <- data.frame(matrix(nrow = length(seqSubset), ncol = maxGroupDepth + 3))  #
set up an object to save the results of the APC; needs 3 more columns than the number of hierarchy
levels defined by maxGroupDepth
```

```
colnames(affiliations) <- c("accession", "affiliation", paste("affil", 0:maxGroupDepth, sep = "0"))  # set the column names

rownames(affiliations) <- colnames(dissimilarityMatrix)  # set rownames identical with colnames of the input identity matrix

affiliations$accession <- rownames(affiliations)  # copy the rownames to the first column of the result matrix

affiliations$affil00 <- 1  # set the initial affiliation level to 1 for all sequences

affiliations$affiliation <- 0  # set the affiliation 0 for all sequences


for(mgd in 0:(maxGroupDepth - 1)) {  # iteratively run through the grouping for all sequences for the given number of hierarchy levels

  prevLevel <- paste("affil", mgd, sep = "0")  # the previous hierarchy level, the starting point for subsetting the dataset

  currLevel <- paste("affil", (mgd + 1), sep = "0")  # the current hierarchy level to be determined for the respective subset of sequences

  affiliations[, currLevel] <- 0  # set the initial affiliations in the currently analysed hierarchy level to the default value

  for(aktSubGroup in unique(affiliations$affiliation[affiliations[,prevLevel] > 0])) {  # run the grouping for the current hierarchy level for all subgroups of the preceding level

    seqSubset <- affiliations$accession[affiliations$affiliation == aktSubGroup]  # generate the list of sequence names belonging to the currently analysed subgroup

    if(length(seqSubset) < aktGroupSize) affiliations[seqSubset, currLevel] <- -1 else {  # check whether the number of sequences in the current group is sufficient according to the preset minimum group size to allow for further subdivision; if not, set the current affiliation -1 to stop further evaluation in the subsequent iterations

      workmat <- as.matrix(dissimilarityMatrix[seqSubset, seqSubset])  # if the current group size allows for further subdivision, get the working matrix only containing data of the relevant subset


      workmatAPC <- apcluster(workmat, details=TRUE, q=0.5)  # calculate the AP-clustering of the current data subset using the default input preference q

      prefRang <- preferenceRange(workmat, exact=TRUE)  # determine the input preference range of the data subset

      pStepWidth <- abs((prefRang[2] - prefRang[1]) / (aktStepNumber - 2))  # adjust the step width to cover the complete input preference range in equal steps

      inPref <- unique(c(prefRang[1], seq(prefRang[1], prefRang[2], pStepWidth), prefRang[2]))  # calculate all input preferences to use in the APC iterations

      plateauWindow <- floor(length(inPref) * winProp)    # set the window size to fit the actual step number and interrogate always the same portion of the overall range

      if(plateauWindow < aktPlateauWindow) plateauWindow <- aktPlateauWindow  # in case the calculated window size for the determination of a cluster number plateau is lower than the preset lower level, adjust the size of the window used to define the plateau to fit with the lower limit

      if(length(inPref) > plateauWindow) {  # test whether sufficient iterations are performed to cover the set window for plateau determination, only start iterating if yes because otherwise an error will occur

        clusTab <- data.frame(inPref, numClust = NA, windowStDev = NA, windowMean = NA, increase = TRUE, stDevOK = TRUE)  # prepare table to save the results of all clustering iterations to enable testing whether or not the stopping criteria are met
```

```
i <- 0  # define counter

stopAPC <- FALSE  # set the control variable

while(i < nrow(clusTab) & stopAPC == FALSE) {  # repeat the calculations for AP clustering of the current data subset until either of the stopping criteria is met

 i <- i + 1  # increase counter for current iteration

 j<-apcluster(workmat, p = clusTab$inPref[i])  # determine the number of AP clusters in the data subset with the given input preference (as previously defined from the preference range and chosen number of iterations)

 clusTab$numClust[i] <- length(j@clusters)  # record the number of AP clusters corresponding with the input preference

 if(i <= plateauWindow) {  # check whether or not sufficient data for calculation of mean and SD from number of clusters is available

  if(i == 1) clusTab$windowStDev[i] <- 0 else clusTab$windowStDev[i] <- sd(clusTab$numClust[1:i])  # if not, set SD of cluster number within window 0 in case of first iteration, otherwise adjust SD calculation to available data instead of preset window

  clusTab$windowMean[i] <- mean(clusTab$numClust[1:i])  # calculate mean from the available data

 } else {  # number of performed iterations higher than window size for plateau definition

  clusTab$windowStDev[i] <- sd(clusTab$numClust[(i - plateauWindow + 1):i])  # calculate SD of cluster number from recent and preceding iterations (in total preset number of iterations)

  clusTab$windowMean[i] <- mean(clusTab$numClust[(i - plateauWindow + 1):i])  # calculate mean cluster number from recent and preceding iterations (in total preset number of iterations)

  clusTab$increase[i] <- clusTab$windowMean[i] >= clusTab$windowMean[(i-1)]  # test whether the number of clusters is the same as or larger than in the preceding iteration, because a decrease is deemed a disruption and leads to termination of the iterative AP clustering

  tempTab <- clusTab[(i - plateauWindow + 1):i,]  # make subset of the table only containing data of the plateauWindow number of rows including the last iteration

  clusTab$stDevOK[i] <- nrow(tempTab[tempTab$windowStDev != 0,]) < plateauWindow  # test whether the SD of the cluster number returns to 0 after an increase of the cluster number (this must be the case if the cluster number is stable for at least plateauWindow iterations), if not a disruption occurred

  stopAPC <- !(clusTab$increase[i] == TRUE & clusTab$stDevOK[i] == TRUE)  # check whether or not both criteria to enter the next iteration, i.e. not to terminate the loop, are fulfilled

 }

}

setIterations <- nrow(clusTab)  # record the set maximum number of iterations

clusTab <- clusTab[1:(i - plateauWindow),]  # cut the table to the number of iterations before the disruption occurred

usedIterations <- nrow(clusTab)  # record the number of iterations with stable plateau

lastStable <- clusTab$numClust[nrow(clusTab)]  # record the number clusters in the last stable plateau

firstPlateau <- min(clusTab$numClust)  # record the number of clusters in the first observed plateau

plateauSummary <- clusTab$numClust   # prepare the identification of the longest plateau
```

```
plateauSummary <- plateauSummary[plateauSummary > firstPlateau]   # only use values higher than the first plateau (as per the definition in Susanne Fischer's paper the first plateau is not valid)

plateauSummary <- summary(as.factor(plateauSummary), maxsum = length(unique(plateauSummary)))  # summarize how often each number of clusters was observed to define the longest plateau, i.e. the number of clusters that was most often observed before the disruption

if(is.element(TRUE, duplicated(plateauSummary))) longestPlateau <- as.numeric(names(plateauSummary[plateauSummary == max(plateauSummary)])) else longestPlateau <- as.numeric(names(which.max(plateauSummary)))   # determine the number of clusters constituting the longest plateau; in case 2 or more cluster numbers are present the same number of iterations, use the higher number of clusters in order not to reduce the cluster number too stringently

allPlateaus <- c(lastStable, longestPlateau)  # concatenate the determined clusternumbers from the longest and the last stable plateau

if(is.element(TRUE, allPlateaus < length(workmatAPC@clusters))) {  # define the best number of clusters to use and record the used choice; the best choice is the highest number of clusters that is equal or lower than the number of clusters determined with the default input preference, therefore, test whether either the last stable or the longest plateau are more stringent than the default

  cutNum <- max(allPlateaus[allPlateaus < length(workmatAPC@clusters)])  # record the number of clusters to use for cutting the tree (below)

  if(cutNum == lastStable) cutCrit <- "last" else cutCrit <- "longest"  # record the choice in case the default is replaced

} else {  # the default value is used

  cutNum <- length(workmatAPC@clusters)  # record the default value of the cluster number to use it for tree cutting below

  cutCrit <- "defaultAPC"  # record the used choice

}


aggdissimilarityMatrix <- aggExCluster(workmat, workmatAPC)   # agglomerative hierarchical clustering

grouping <- cutree(aggdissimilarityMatrix, k = cutNum)    # cutting the tree to determine the resulting grouping of sequences; k = number of groups to have = cluster number as determined above


if(length(grouping@clusters) == 1)  for(g in 1:length(grouping@clusters)) affiliations[rownames(workmat)[grouping@clusters[[g]]], currLevel] <- -3 else for(g in 1:length(grouping@clusters)) affiliations[rownames(workmat)[grouping@clusters[[g]]], currLevel] <- g  # record the grouping in the current subset of the current hierarchical level; in case the subset cannot be further subdivided (number of clusters is 1), record -3 to label the grouping being terminated for the subset because it cannot be further subdivided; in all other cases, record the group affiliations per sequence

 } else affiliations[seqSubset, currLevel] <- -2  # in case there is not enough steps for the calculations, report -2 to label the subgroup for subsequent cycles and error analysis

}

## in the following lines, record all current settings of the iteration

paramCollection$terminatingInPref[nrow(paramCollection)] <- clusTab$inPref[nrow(clusTab)]

paramCollection$level[nrow(paramCollection)] <- mgd
```

```
            paramCollection$group[nrow(paramCollection)] <- aktSubGroup
            paramCollection$inputGroupSize[nrow(paramCollection)] <- length(seqSubset)
            paramCollection$usedStepWidth[nrow(paramCollection)] <- pStepWidth
            paramCollection$setIterations[nrow(paramCollection)] <- setIterations
            paramCollection$usedIterations[nrow(paramCollection)] <- usedIterations
            paramCollection$minPrefRange[nrow(paramCollection)] <- prefRang[1]
            paramCollection$maxPrefRange[nrow(paramCollection)] <- prefRang[2]
            paramCollection$lastStable[nrow(paramCollection)] <- lastStable
            if(length(longestPlateau > 0)) paramCollection$longest[nrow(paramCollection)] <- longestPlateau else paramCollection$longest[nrow(paramCollection)] <- NA
            paramCollection$defaultAPC[nrow(paramCollection)] <- length(workmatAPC@clusters)
            paramCollection$cutCrit[nrow(paramCollection)] <- cutCrit
            paramCollection$usedWindowSize[nrow(paramCollection)] <- plateauWindow
            paramCollection <- rbind(paramCollection, NA) # add the next line to the table to accommodate the data of the next iteration
            ## End parameter recording

            ## in the following lines, record all results of the current iteration
            allResults$group <- append(allResults$group, aktSubGroup)
            allResults$defaultAPresult <- append(allResults$defaultAPresult, workmatAPC)
            allResults$aggExResult <- append(allResults$aggExResult, aggdissimilarityMatrix)
            allResults$cutreeResult <- append(allResults$cutreeResult, grouping)
            ## End results recording
          }
          if(mgd == 0) affiliations$affiliation[affiliations[, currLevel] > 0] <- affiliations[affiliations[, currLevel] > 0, currLevel] else affiliations$affiliation[affiliations[, currLevel] > 0] <- paste(affiliations$affiliation[affiliations[, currLevel] > 0], affiliations[affiliations[, currLevel] > 0, currLevel], sep = ".")  # construct the overall group designation from the previously present portion and the currently analyzed hierarchy level; in case it is the first level iteration, replace the present values with the current
        }
        affiliations$affil00 <- NULL  # delete the initial grouping

        ## save results to disk
        write_xlsx(affiliations, filename)
        write_xlsx(paramCollection, sub("Affiliations", "usedParameters", filename))
        save.image(file = sub("Affiliations", "CompleteData", sub("xlsx", "RData", filename)))
      }
    }
  }
 }
} else print("Please check the column and row names in your input file! They must be identical!")
```

Figure S1. Geographic distribution of WNV cases in Germany in 2020 (depicted on district level) as shown in A. Specific areas with WNV cases in the areas of Saxony, Saxony-Anhalt, Thuringia, Berlin and Brandenburg were shown in B and WNV cases in Berlin and surrounding areas in Brandenburg were shown in C. Blue squares and red circles indicate notifiable WNV cases of horses and birds. WNV cases with numbers indicated that these samples were subjected to whole-genome sequencing. WNV cases that were not selected for sequencing (e.g., IgM-positive cases or high C_q values) remain unnumbered. Intensity of the colored background at district level indicates the frequency, how often an area was affected by WNV activity in prior years.

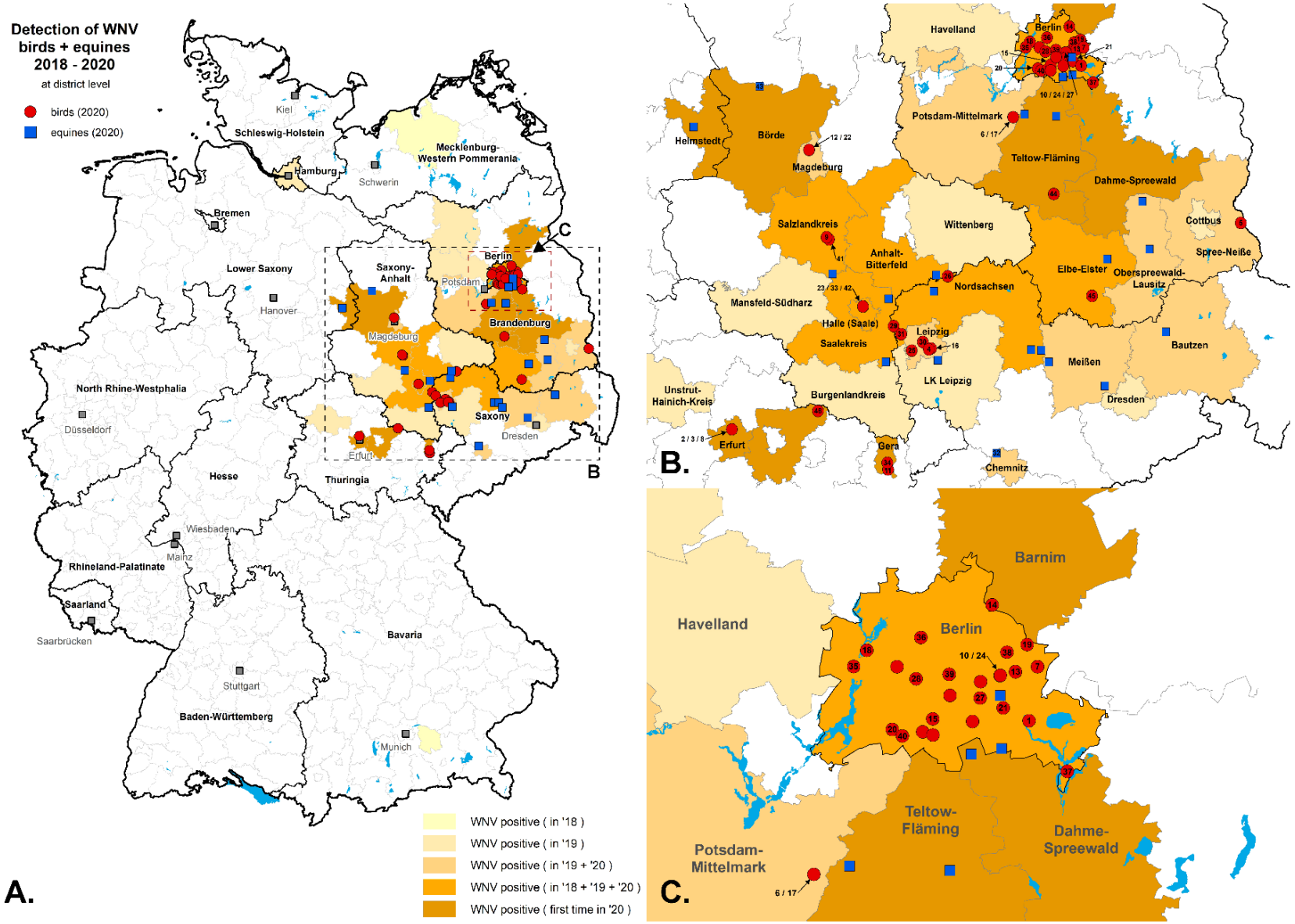
Detection of WNV
birds + equines
2018 - 2020
at district level
birds (2020)
equines (2020)
Kiel
Schleswig-Holstein
Hamburg
Mecklenburg-
Western Pommerania
Schwerin
Bremen
Lower Saxony
Hanover
Saxony-
Anhalt
Potsdam
Berlin
Brandenburg
Magdeburg
Saxony
Dresden
Erfurt
Thuringia
North Rhine-Westphalia
Düsseldorf
Hesse
Wiesbaden
Mainz
Rhineland-Palatinate
Saarland
Saarbrücken
Bavaria
Stuttgart
Baden-Württemberg
Munich
A.
B
C
WNV positive (in '18)
WNV positive (in '19)
WNV positive (in '19 + '20)
WNV positive (in '18 + '19 + '20)
WNV positive (first time in '20)
Havelland
Berlin
Potsdam-Mittelmark
6 / 17
Helmstedt
Börde
12 / 22
Magdeburg
Teltow-Fläming
Dahme-Spreewald
Salzlandkreis
Wittenberg
Cottbus
Spree-Neiße
Anhalt-
Bitterfeld
Elbe-Elster
Oberspreewald-
Lausitz
Nordsachsen
Mansfeld-Südharz
23 / 33 / 42
Halle (Saale)
Saalekreis
Leipzig
Bautzen
Meißen
Unstrut-
Hainich-Kreis
Burgenlandkreis
LK Leipzig
Dresden
2 / 3 / 8
Erfurt
Gera
Chemnitz
B.
Barnim
Havelland
Berlin
10 / 24
Teltow-
Fläming
Dahme-
Spreewald
Potsdam-
Mittelmark
6 / 17
C.

Figure S2 Climatological maps of Germany displaying A) temperature (in degree celsius), B) precipitation (in millimeter) and C) water balance (in millimeter) based on data collected in summer 2020. Climatological maps were downloaded from Deutscher Wetterdienst; https://www.dwd.de/EN/climate_environment/climatemonitoring/germany/germany_node.html (Deutscher Wetterdienst 2020)

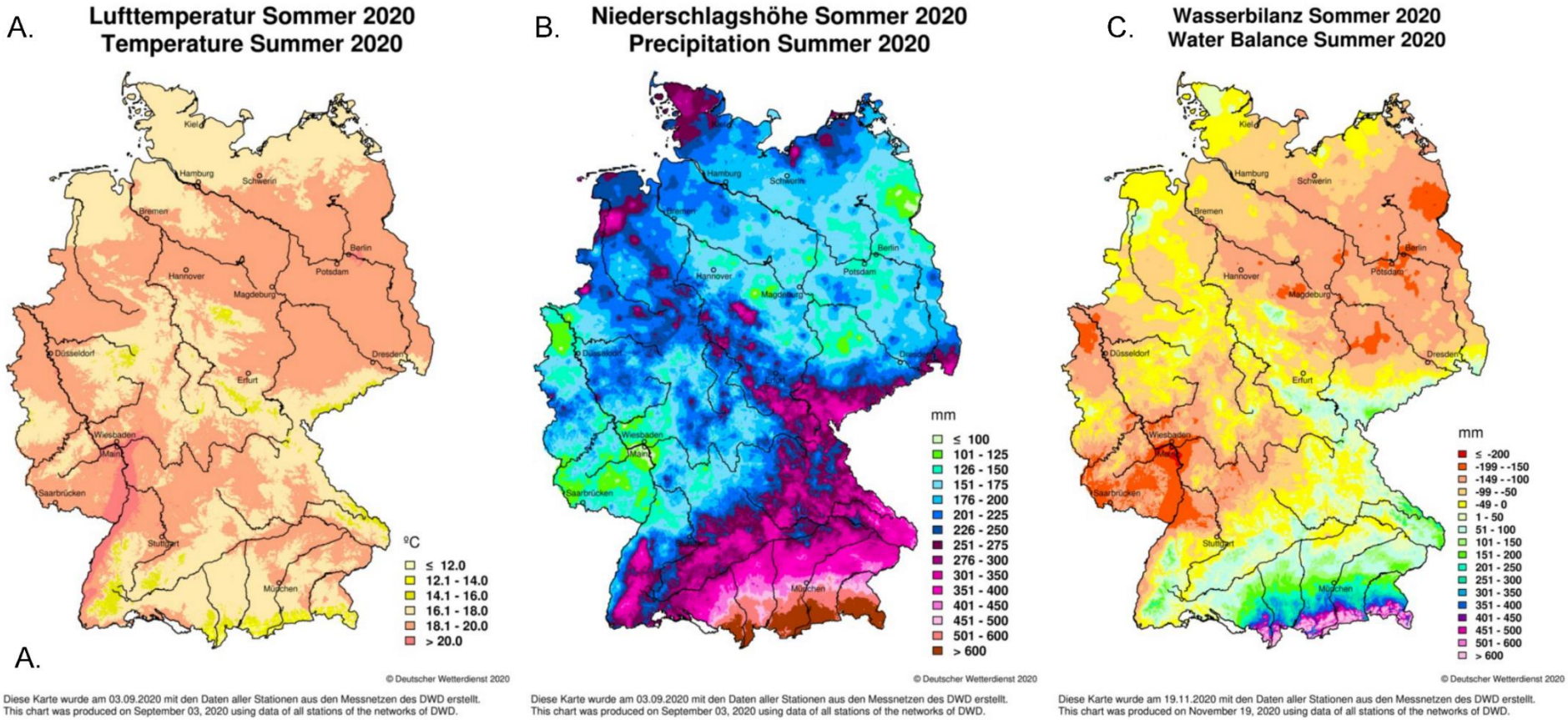

Deutscher Wetterdienst (2021), 'Climatological maps of Germany',
<https://www.dwd.de/EN/ourservices/klimakartendeutschland/klimakartendeutschland.html?nn=495490>, accessed 15.07.2021.

Table S1 West Nile Virus primer sequences from Sikkema et al. 2020. Each primer stock was normalized to 100 micromolar concentration. Volumes of each primer per primer mix (mix 1 or 2) were specified in the table below. These primers mixes were then subjected to 1:10 dilution.

Primer number	Mix	Primer	Primer sequence	Used volume (µl)
1	1	WNVUS1_1_LEFT	GCCTGTGTGARCTGACAAACTTAG	10
2	1	WNVUS1_1_RIGHT	CTTTTCTTTTGTTTTGRGCTCCG	10
3	1	WNVUS1_3_LEFT	AGTTACCCTCTCTAACTTCCAAG	15
4	1	WNVUS1_3_LEFT_2	GTGACCCTCTCCAACTTCCAGG	15
5	1	WNVUS1_3_RIGHT	CARGAAGTCTCTGTTRCTCATTCC	15
6	1	WNVUS1_5_LEFT_2	GTGTCCAACCATGGGTGAAGCC	10
7	1	WNVUS1_5_LEFT	GCCCGACCATGGGAGAAGCT	10
8	1	WNVUS1_5_RIGHT_2	GTGGCATGAGGTTCTTCAAACTCC	10
9	1	WNVUS1_5_RIGHT	GGCGTGTGGTTCCTCAAACTCC	10
10	1	WNVUS1_7_LEFT_2	TCTGAAGTGTAGGGTGAAGATGGAG	10
11	1	WNVUS1_7_LEFT	GTCATTTGAAGTGTAGAGTGAAGATGG	10
12	1	WNVUS1_7_RIGHT	GAGGTGAAMACCCCTCCAACTG	10
13	1	WNVUS1_9_LEFT	GTGGATGGGMATCAATGCYCGT	10
14	1	WNVUS1_9_RIGHT_2	CTCTTGCCCCAAGCCTTCCAAC	10
15	1	WNVUS1_9_RIGHT	CTTTCCCCAGGCCTTCCAGC	10
16	1	WNVUS1_11_LEFT	CACAACKGAATGYGACTCGAAGAT	10
17	1	WNVUS1_11_RIGHT	ACGGTGTCCGCAGCTCTCAC	10
18	1	WNVUS1_11_RIGHT_2	CACGGTGTCCGCAACTRTCAC	10
19	1	WNVUS1_13_LEFT_2	GGCACGACGAAAAGACCCTCGTGC	10
20	1	WNVUS1_13_LEFT	GACATGATGAAAAGACCCTCGTGC	10
21	1	WNVUS1_13_RIGHT_2	CTCTTGGTTGGTCCACCTTGC	10
22	1	WNVUS1_13_RIGHT	CTCCTGGTTGGTCCATCTCGC	10
23	1	WNVUS1_15_LEFT_2	CAAATGTGGTGGTGCCGCTGC	10
24	1	WNVUS1_15_LEFT	CGACATCAAACGTGGTTGTTCCG	10
25	1	WNVUS1_15_RIGHT_2	CYGTCCTCTCAATCCACATGTC	10
26	1	WNVUS1_15_RIGHT	CGCCGTTCTCTCAATCCACATATC	10
27	1	WNVUS1_17_LEFT_2	ATAAGTGCCTACACACCYTGGGC	10
28	1	WNVUS1_17_LEFT	GGAARATATGGATGCTCAGAATGG	10
29	1	WNVUS1_17_RIGHT_2	CCCCAATTTCTCCTTCTGGTGTC	10
30	1	WNVUS1_17_RIGHT	TTTGAACACCCCTGGTTTCGTC	10
31	1	WNVUS1_19_LEFT_2	CCATTGTGCAAGGAGAGAGAATGG	10
32	1	WNVUS1_19_LEFT	CGGATTCGAACCTGAGATGCTG	10
33	1	WNVUS1_19_RIGHT_2	CGATGCTCGCTGGATCCGTG	10
34	1	WNVUS1_19_RIGHT	CATGAATATTGCCGCCGCCTC	10
35	1	WNVUS1_21_LEFT_2	GGAAAGACCGTTTGGTTTGTTCC	10
36	1	WNVUS1_21_LEFT	GGGAAGACGGTTTGGTTTGTGC	10
37	1	WNVUS1_21_RIGHT_2	GAGTCGTCTTCATTCGTGTGCC	10
38	1	WNVUS1_21_RIGHT	GTTGGAATCATCCTCATTTGTGTGC	10
39	1	WNVUS1_23_LEFT	CGGCTGGAGTGTCATACCACG	10
40	1	WNVUS1_23_LEFT_2	CAGCAGGAATATCATACCATGACC	10
41	1	WNVUS1_23_RIGHT_2	CTATTGTCTGAAGGGCGTCCGG	10

Primer number	Mix	Primer	Primer sequence	Used volume (µl)
42	1	WNVUS1_23_RIGHT	GAATACTCCCATGGTCATCACACTC	10
43	1	WNVUS1_25_LEFT_2	CAGGAACGAAAATAGCAGGCATGC	10
44	1	WNVUS1_25_LEFT	GGAACGAAGATCGCCGGAATG	10
45	1	WNVUS1_25_RIGHT_2	GCTTCCGCTTGCCAGCCTG	10
46	1	WNVUS1_25_RIGHT	GCTGAGCGCATTGCCTCAGC	10
47	1	WNVUS1_27_LEFT_2	CAGTCATGCAGAAAAARGTTGGACAG	10
48	1	WNVUS1_27_LEFT	GATCTTGGTGTCTCTAGCTGCAG	10
49	1	WNVUS1_27_RIGHT_2	CGAGATCCACAACCTTTCCCAC	10
50	1	WNVUS1_27_RIGHT	CATCCAAGGTCAATCACTTTTCCG	10
51	1	WNVUS1_29_LEFT_2	CTGGCCATGAAGAGCCACAAC	10
52	1	WNVUS1_29_LEFT	GTACAGGAAGTGAAAGGGTACACG	10
53	1	WNVUS1_29_RIGHT_2	GTTGACATCTTCCTCAAACTGGGG	10
54	1	WNVUS1_29_RIGHT	GCCCTGGTTCCACTTCCCAAG	10
55	1	WNVUS1_31_LEFT_2	GAATACAGCTCCACATGGCACC	10
56	1	WNVUS1_31_LEFT	GAGAACCACCCATATAGAACCTGG	10
57	1	WNVUS1_31_RIGHT	CTCTTTCCCATCATGTTGTARATGC	10
58	1	WNVUS1_33_LEFT_2	GGGTACATCTTGAAGGAAGTYGG	10
59	1	WNVUS1_33_LEFT	GTTACATCCTGCGTGAAGTTGGC	10
60	1	WNVUS1_33_RIGHT	CSCCATTCTCAAACAGCCAGG	10
61	1	WNVUS1_35_LEFT_2	GGTGGTATGACTGGCAGCAGG	10
62	1	WNVUS1_35_LEFT	GATGGTATGATTGGCAGCAGGTTC	10
63	1	WNVUS1_35_RIGHT	GTCTTCCATCCAYTCATTCTCCTC	10
64	1	WNVUS1_37_LEFT	GAGAAGTATGYGGATTACATGAGYTC	15
65	1	WNVUS1_37_RIGHT	GGTCTCCTCTAACCTCTAGTCC	15
66	2	WNVUS1_2_RIGHT_2	CGGGCTGTCAATATGCTAAAACGC	10
67	2	WNVUS1_2_RIGHT	GTGCACCAGCAGTCAATGTCTTC	10
68	2	WNVUS1_2_LEFT	GTGCACCAACAGTCGATGTCTTC	10
69	2	WNVUS1_4_LEFT	GGATGCTAGGAAGCAACACAATGC	10
70	2	WNVUS1_4_RIGHT_2	GATGCTTGGRAGCAACACCATG	10
71	2	WNVUS1_4_RIGHT	TGCTYCCCTTTCCAAACAGTCC	10
72	2	WNVUS1_4_LEFT_2	GCTTCCTTTGCCAAATAGTCCGC	10
73	2	WNVUS1_6_LEFT	GACTGTGARCCACGGTCAGG	10
74	2	WNVUS1_6_RIGHT_2	CCGGTGTATTGCAGTTCCAACAC	10
75	2	WNVUS1_6_RIGHT	GCAATTCCAACACCACAGTGCC	10
76	2	WNVUS1_8_LEFT_2	GTGAATCCATTTGTGTCTGTGGCC	10
77	2	WNVUS1_8_LEFT	GTCAACCCTTTTGTTTCAGTGGCC	10
78	2	WNVUS1_8_RIGHT_2	GATCCATCCAGGCTTCCACATC	10
79	2	WNVUS1_8_RIGHT	GGTCCATCCAAGCCTCCACATC	10
80	2	WNVUS1_10_LEFT_2	AGACTCGAGCACCAAATGTGGG	10
81	2	WNVUS1_10_LEFT	CCAGACTGGAGCATCAAATGTGG	10
82	2	WNVUS1_10_RIGHT	GAACYGCCCTYTCAAGCTTCC	10
83	2	WNVUS1_12_LEFT	GAAGTYAAATCATGYACSTGGCC	10
84	2	WNVUS1_12_RIGHT	CTTGCGAAGGACCTCCTGGG	10
85	2	WNVUS1_14_LEFT_2	GTCCTAGTGTTTGGGGGTATTACG	10
86	2	WNVUS1_14_LEFT	CCTGGTGTTTGGGGGCATTAC	10
87	2	WNVUS1_14_RIGHT_2	GCAGATGAGGCAAGCYCCTTTC	10

Primer number	Mix	Primer	Primer sequence	Used volume (µl)
88	2	WNVUS1_14_RIGHT	CAAGCATARCAGACTTGCTCCTTTC	10
89	2	WNVUS1_16_LEFT_2	CTGCAGTTGGACTCATGTTTGCC	10
90	2	WNVUS1_16_LEFT	GCTGTCGGCYTRATGTTTGCCA	10
91	2	WNVUS1_16_RIGHT_2	GGTGATGGTGTGTCCCAAAGRAC	10
92	2	WNVUS1_16_RIGHT	GAGGGAGTGTCCCACARCAC	10
93	2	WNVUS1_18_LEFT_2	CCACACACTATGGCACACCAC	10
94	2	WNVUS1_18_LEFT	GCAGGAGCRGGCGTGATG	10
95	2	WNVUS1_18_RIGHT_2	CTCARTCTTTTGTTGATGGCCTCC	10
96	2	WNVUS1_18_RIGHT	GCCACAGATCATCAAAGAGGCC	10
97	2	WNVUS1_20_LEFT_2	GATGTCTCCACACAGAGTCCC	10
98	2	WNVUS1_20_LEFT	GATGTCTCCTCACAGGGTGCC	10
99	2	WNVUS1_20_RIGHT_2	GAAAGTCGTAYGAGACGGAGTAC	10
100	2	WNVUS1_20_RIGHT	GGGTACTCTGTCTCATAGGACTTTC	10
101	2	WNVUS1_22_LEFT_2	GCTCAGCGGAGAGGACGC	10
102	2	WNVUS1_22_LEFT	CGCCCAGAGACGTGGACG	10
103	2	WNVUS1_22_RIGHT_2	CTTTCTCTCACCCAACTTCGTG	10
104	2	WNVUS1_22_RIGHT	GGCCTCAGAATCTTCCTTTCACC	10
105	2	WNVUS1_24_LEFT_2	GATCACAAATCGGGCTCGTTGAG	10
106	2	WNVUS1_24_LEFT	CGTTCTCAGATAGGGCTCATTGAG	10
107	2	WNVUS1_24_RIGHT_2	CAACTCCCAGRGTCGTCTCTC	10
108	2	WNVUS1_24_RIGHT	CTCCTTGACCTCAATTCTTTGCCC	10
109	2	WNVUS1_26_LEFT_2	GTGGACGTTGGTGTGTCAGCTC	10
110	2	WNVUS1_26_LEFT	CTTCGTCGATGTTGGAGTGTCG	10
111	2	WNVUS1_26_RIGHT_2	GTTGCATTCCACACTGAACTAGC	10
112	2	WNVUS1_26_RIGHT	CCAAACAGAGCTTGCTCCATTCTC	10
113	2	WNVUS1_28_LEFT_2	GGGAAGTTTGGAAGGAGAGACTC	10
114	2	WNVUS1_28_LEFT	GTACCGCAAAGAGGCCATCATC	10
115	2	WNVUS1_28_RIGHT_2	CCAATGTCACAGAGCAGTGTGTC	10
116	2	WNVUS1_28_RIGHT	GARGACTCTCCGATGTCACAAAG	10
117	2	WNVUS1_30_LEFT_2	CCATGAGATGTACTGGGTGAGY	15
118	2	WNVUS1_30_LEFT	GACTGGTCAGAAACCCACTCTC	15
119	2	WNVUS1_30_RIGHT_2	GAAGGGAGTAGTGTCAGTCATGG	15
120	2	WNVUS1_30_RIGHT	CACTCGTTGTTGACCGAAAGGAG	15
121	2	WNVUS1_32_LEFT_2	GGAAGAACGCCCGGGAAGC	10
122	2	WNVUS1_32_LEFT	GAGGAGCGCCAGAGARGCAG	10
123	2	WNVUS1_32_RIGHT_2	CAGCAGTTCAAGAACCTTCGCTTC	10
124	2	WNVUS1_32_RIGHT	CCAAGTCAGCTCTCGTGATGCG	10
125	2	WNVUS1_34_LEFT_2	GTGAAAGTGATGCGCCCGGC	10
126	2	WNVUS1_34_LEFT	GTCGTGAAAGTGATGAGGCCAG	10
127	2	WNVUS1_34_RIGHT_2	GAGAWATGCGAGCTCTGCCTAC	10
128	2	WNVUS1_34_RIGHT	CGCACATTCCATCCAGCCCC	10
129	2	WNVUS1_36_LEFT_2	CGCAAAAGGAGAATGGATGACGAC	10
130	2	WNVUS1_36_LEFT	CCATGCAGGAGGAGAGTGGATG	10
131	2	WNVUS1_36_RIGHT	CGTCTACTCAACTTCCGGTGG	10
132	2	WNVUS1_38_LEFT	CCCTCAGAACCGTCTCGGAAG	10
133	2	WNVUS1_38_RIGHT	GCACTGTGCCGTGTGGCTG	10

Table S2 Samples used to validate the WNV multiplex PCR High-throughput sequencing (HTS) in comparison with the result of unbiased and direct HTS approach.

Sample			Reference sequence				This study			Result of sequence comparison
Code	ID	Cq value	Library ID	applied protocol	INSDC Accesssion	Length (nt)	Library ID	INSDC Accesssion	Length (nt)	
C1	ED-I-62/19	22.9	lib03378	Wylezich et al 2018	LR743425	11,060	lib04562	XX	10,989	identical
C2	ED-I-156/19	11.8	lib03418	Wylezich et al 2018	LR743423	11,027	lib04563	XX	10,989	Identical
C3	ED-I-155/19	17.5	lib03420	Wylezich et al 2018	LR743422	11,010	lib04564	XX	10,987	Identical
C4	ED-I-115/19	31.5	lib03988	Wylezich et al 2021	LR989891	6,470	lib04565	XX	10,989	8 substitutions[1]
C5	ED-I-127-18	29.4	lib03224	Wylezich et al 2021	Unpublished	6,786	lib04748	XX	10,988	2 substitutions[1]

[1] based on available partial reference sequence; insertions and deletions not considered

Table S3 List of full genome sequences retrieved from Genbank

Accession number	Used in Dataset
DQ116961	WL2
HQ537483	WL2
JN858070	WL2
KC407673	WL2
KC496015	WL2
KC496016	WL2
KF179639	WL2
KF179640	WL2
KF588365	WL2
KF647249	WL2
KF647250	WL2
KF647251	WL2
KF647252	WL2
KF823806	WL2
KJ577738	WL2
KJ577739	WL2
KJ883342	WL2
KJ883343	WL2
KJ883344	WL2
KJ883345	WL2
KJ883346	WL2
KJ883348	WL2
KJ883349	WL2
KJ883350	WL2
KM203860	WL2
KM203861	WL2
KM203862	WL2
KM203863	WL2
KM659876	WL2
KP109691	WL2
KP109692	WL2
KP780837	WL2
KP780838	WL2
KP780839	WL2
KP789953	WL2
KP789954	WL2
KP789955	WL2
KP789956	WL2
KP789957	WL2
KP789958	WL2
KP789959	WL2
KP789960	WL2
KT207792	WL2
KT359349	WL2
KT757318	WL2

Accession number	Used in Dataset
KT757319	WL2
KT757320	WL2
KT757321	WL2
KT757322	WL2
KT757323	WL2
KU206781	WL2
KU573080	WL2
KU573081	WL2
KU573082	WL2
KU573083	WL2
KX375812	WL2
KY594040	WL2
LR743421	WL2
LR743422	WL2
LR743423	WL2
LR743424	WL2
LR743425	WL2
LR743426	WL2
LR743427	WL2
LR743428	WL2
LR743429	WL2
LR743430	WL2
LR743431	WL2
LR743432	WL2
LR743433	WL2
LR743434	WL2
LR743435	WL2
LR743436	WL2
LR743437	WL2
LR743442	WL2
LR743443	WL2
LR743444	WL2
LR743445	WL2
LR743446	WL2
LR743447	WL2
LR743448	WL2
LR743449	WL2
LR743450	WL2
LR743451	WL2
LR743452	WL2
LR743453	WL2
LR743454	WL2
LR743455	WL2
LR743456	WL2
LR743457	WL2
LR743458	WL2

Accession number	Used in Dataset
LR989885	WL2
LR989888	WL2
MF984337	WL2
MF984338	WL2
MF984339	WL2
MF984340	WL2
MF984341	WL2
MF984342	WL2
MF984343	WL2
MF984344	WL2
MF984345	WL2
MF984346	WL2
MF984347	WL2
MF984348	WL2
MF984349	WL2
MF984350	WL2
MF984351	WL2
MF984352	WL2
MH021189	WL2
MH244510	WL2
MH244511	WL2
MH244512	WL2
MH244513	WL2
MH549209	WL2
MH910045	WL2
MH924836	WL2
MH986055	WL2
MH986056	WL2
MK473443	WL2
MK947396	WL2
MK947397	WL2
MN480792	WL2
MN480793	WL2
MN480794	WL2
MN480795	WL2
MN481589	WL2
MN481590	WL2
MN481591	WL2
MN481592	WL2
MN481593	WL2
MN481594	WL2
MN481595	WL2
MN481596	WL2
MN481597	WL2
MN652878	WL2
MN652879	WL2

Accession number	Used in Dataset
MN652880	WL2
MN794935	WL2
MN794937	WL2
MN794938	WL2
MN794939	WL2
MN939557	WL2
MN939558	WL2
MN939559	WL2
MN939560	WL2
MN939561	WL2
MN939562	WL2
MN939562	WL2
MN939564	WL2
MT341470	WL2
MT341471	WL2
MT341472	WL2
MT863560	WL2
MT863561	WL2
MW036634	WL2
MW142223	WL2
MW142224	WL2
MW142226	WL2
MW142227	WL2
AF196835	TD01 / TD03
AY277251	TD01 / TD03
AY532665	TD01 / TD03
AY701412	TD01 / TD03
AY701413	TD01 / TD03
AY765264	TD01 / TD03
DQ176636	TD01 / TD03
DQ256376	TD01 / TD03
DQ786573	TD01 / TD03
EF429197	TD01 / TD03
EF429198	TD01 / TD03
EF429199	TD01 / TD03
EF429200	TD01 / TD03
EU082200	TD01 / TD03
EU249803	TD01 / TD03
FJ159129	TD01 / TD03
FJ159130	TD01 / TD03
FJ159131	TD01 / TD03
FJ425721	TD01 / TD03
FJ483548	TD01 / TD03
FJ483549	TD01 / TD03
FJ766331	TD01 / TD03
FJ766332	TD01 / TD03

Accession number	Used in Dataset
GQ379161	TD01 / TD03
GQ851602	TD01 / TD03
GQ851603	TD01 / TD03
GQ851604	TD01 / TD03
GQ851605	TD01 / TD03
GQ851606	TD01 / TD03
GQ851607	TD01 / TD03
GQ903680	TD01 / TD03
GU011992	TD01 / TD03
HM051416	TD01 / TD03
HM147822	TD01 / TD03
HM147823	TD01 / TD03
HM147824	TD01 / TD03
HM152775	TD01 / TD03
HQ537483	TD01 / TD03
JF707789	TD01 / TD03
JF719066	TD01 / TD03
JF719067	TD01 / TD03
JF719068	TD01 / TD03
JF719069	TD01 / TD03
JN393308	TD01 / TD03
JN858069	TD01 / TD03
JN858070	TD01 / TD03
JQ928174	TD01 / TD03
JQ928175	TD01 / TD03
JX041628	TD01 / TD03
JX041629	TD01 / TD03
JX041630	TD01 / TD03
JX041632	TD01 / TD03
JX041634	TD01 / TD03
JX123030	TD01 / TD03
JX123031	TD01 / TD03
JX442279	TD01 / TD03
JX556213	TD01 / TD03
KC407673	TD01 / TD03
KC496015	TD01 / TD03
KC496016	TD01 / TD03
KC601756	TD01 / TD03
KC954092	TD01 / TD03
KF179639	TD01 / TD03
KF179640	TD01 / TD03
KF234080	TD01 / TD03
KF647251	TD01 / TD03
KF647253	TD01 / TD03
KJ831223	TD01 / TD03
KJ883346	TD01 / TD03

Accession number	Used in Dataset
KJ934710	TD01 / TD03
KM052152	TD01 / TD03
KM203861	TD01 / TD03
KM203862	TD01 / TD03
KM203863	TD01 / TD03
KP109692	TD01 / TD03
KP780837	TD01 / TD03
KP780838	TD01 / TD03
KP780839	TD01 / TD03
KP780840	TD01 / TD03
KT163243	TD01 / TD03
KT207791	TD01 / TD03
KT207792	TD01 / TD03
KT359349	TD01 / TD03
KT934796	TD01 / TD03
KT934797	TD01 / TD03
KT934798	TD01 / TD03
KT934799	TD01 / TD03
KT934800	TD01 / TD03
KT934801	TD01 / TD03
KT934802	TD01 / TD03
KT934803	TD01 / TD03
KU588135	TD01 / TD03
KY703854	TD01 / TD03
KY703855	TD01 / TD03
KY703856	TD01 / TD03
AF196835	TD02 / TD03
AF202541	TD02 / TD03
AF206518	TD02 / TD03
AF260967	TD02 / TD03
AF260968	TD02 / TD03
AF260969	TD02 / TD03
AF317203	TD02 / TD03
AF404753	TD02 / TD03
AF404754	TD02 / TD03
AF404755	TD02 / TD03
AF404756	TD02 / TD03
AF404757	TD02 / TD03
AF481864	TD02 / TD03
AF533540	TD02 / TD03
AJ965626	TD02 / TD03
AJ965628	TD02 / TD03
AM404308	TD02 / TD03
AY262283	TD02 / TD03
AY268132	TD02 / TD03
AY268133	TD02 / TD03

Accession number	Used in Dataset
AY274504	TD02 / TD03
AY277252	TD02 / TD03
AY278441	TD02 / TD03
AY278442	TD02 / TD03
AY289214	TD02 / TD03
AY603654	TD02 / TD03
AY646354	TD02 / TD03
AY660002	TD02 / TD03
AY701412	TD02 / TD03
AY701413	TD02 / TD03
AY712945	TD02 / TD03
AY712946	TD02 / TD03
AY712947	TD02 / TD03
AY712948	TD02 / TD03
AY795965	TD02 / TD03
DQ005530	TD02 / TD03
DQ080051	TD02 / TD03
DQ080052	TD02 / TD03
DQ080053	TD02 / TD03
DQ080054	TD02 / TD03
DQ080055	TD02 / TD03
DQ080056	TD02 / TD03
DQ080057	TD02 / TD03
DQ080058	TD02 / TD03
DQ080059	TD02 / TD03
DQ080060	TD02 / TD03
DQ080061	TD02 / TD03
DQ080062	TD02 / TD03
DQ080063	TD02 / TD03
DQ080064	TD02 / TD03
DQ080065	TD02 / TD03
DQ080066	TD02 / TD03
DQ080067	TD02 / TD03
DQ080068	TD02 / TD03
DQ080069	TD02 / TD03
DQ080070	TD02 / TD03
DQ080071	TD02 / TD03
DQ080072	TD02 / TD03
DQ118127	TD02 / TD03
DQ164186	TD02 / TD03
DQ164187	TD02 / TD03
DQ164188	TD02 / TD03
DQ164189	TD02 / TD03
DQ164190	TD02 / TD03
DQ164191	TD02 / TD03
DQ164192	TD02 / TD03

Accession number	Used in Dataset
DQ164193	TD02 / TD03
DQ164194	TD02 / TD03
DQ164195	TD02 / TD03
DQ164196	TD02 / TD03
DQ164197	TD02 / TD03
DQ164198	TD02 / TD03
DQ164199	TD02 / TD03
DQ164200	TD02 / TD03
DQ164201	TD02 / TD03
DQ164202	TD02 / TD03
DQ164203	TD02 / TD03
DQ164204	TD02 / TD03
DQ164205	TD02 / TD03
DQ164206	TD02 / TD03
DQ176637	TD02 / TD03
DQ211652	TD02 / TD03
DQ256376	TD02 / TD03
DQ374650	TD02 / TD03
DQ374651	TD02 / TD03
DQ374652	TD02 / TD03
DQ374653	TD02 / TD03
DQ377178	TD02 / TD03
DQ377179	TD02 / TD03
DQ377180	TD02 / TD03
DQ411029	TD02 / TD03
DQ411030	TD02 / TD03
DQ411031	TD02 / TD03
DQ411032	TD02 / TD03
DQ411033	TD02 / TD03
DQ411034	TD02 / TD03
DQ411035	TD02 / TD03
DQ431693	TD02 / TD03
DQ431694	TD02 / TD03
DQ431695	TD02 / TD03
DQ431696	TD02 / TD03
DQ431697	TD02 / TD03
DQ431698	TD02 / TD03
DQ431699	TD02 / TD03
DQ431700	TD02 / TD03
DQ431701	TD02 / TD03
DQ431702	TD02 / TD03
DQ431703	TD02 / TD03
DQ431704	TD02 / TD03
DQ431705	TD02 / TD03
DQ431706	TD02 / TD03
DQ431707	TD02 / TD03

Accession number	Used in Dataset
DQ431708	TD02 / TD03
DQ431709	TD02 / TD03
DQ431710	TD02 / TD03
DQ431711	TD02 / TD03
DQ431712	TD02 / TD03
DQ666448	TD02 / TD03
DQ666449	TD02 / TD03
DQ666450	TD02 / TD03
DQ666451	TD02 / TD03
DQ666452	TD02 / TD03
DQ786572	TD02 / TD03
DQ786573	TD02 / TD03
EU249803	TD02 / TD03
FJ483548	TD02 / TD03
FJ483549	TD02 / TD03
FJ527738	TD02 / TD03
FJ766331	TD02 / TD03
FJ766332	TD02 / TD03
GQ379157	TD02 / TD03
GQ379158	TD02 / TD03
GQ379159	TD02 / TD03
GQ379160	TD02 / TD03
GQ379161	TD02 / TD03
GQ851602	TD02 / TD03
GQ851603	TD02 / TD03
GQ851604	TD02 / TD03
GQ851605	TD02 / TD03
GQ851606	TD02 / TD03
GQ851607	TD02 / TD03
GQ851608	TD02 / TD03
GU011992	TD02 / TD03
GU827998	TD02 / TD03
GU827999	TD02 / TD03
GU828000	TD02 / TD03
GU828001	TD02 / TD03
GU828002	TD02 / TD03
GU828003	TD02 / TD03
GU828004	TD02 / TD03

Table S4 Summary and comparison of parameter values from Beast analysis, parts A and B

(A) Result of marginal likelihood (log) estimation path sampling and stepping stone sampling methods for West Nile Virus Lineage 2 dataset using different coalescent models, and strict and uncorrelated relaxed log normal molecular clock models. (B) Calculation of best coalescent model and molecular clock model using Bayes factor. Bayes factor range 1-3 means hardly worth mentioning, 3-20 means postive support, 20-150 means strong support and >150 overwhelming support.

	Dataset	Sampling	Evolutionary Model	Strict	Uncorrelated relaxed log normal
Part A	European WNV Lineage 2 complete coding sequences	Stepping stone sampling	Constant	-29244.94581	-29221.69928
			GMRF SkyRide	-29247.67687	-29221.64373
			Bayesian SkyGrid	-29245.38443	-29215.06113
		Path Sampling	Constant	-29248.94892	-29218.79735
			GMRF SkyRide	-29243.10843	-29216.66507
			Bayesian SkyGrid	-29242.2842	-29211.11923

				Strict			Uncorrelated relaxed log normal		
				Constant	GMRF SkyRide	Bayesian SkyGrid	Constant	GMRF SkyRide	Bayesian SkyGrid
Part B	Stepping stone sampling	Strict	Constant	0.00	-2.73	-0.44	23.25	23.30	29.88
			GMRF SkyRide	2.73	0.00	2.29	25.98	26.03	32.62
			Bayesian SkyGrid	0.44	-2.29	0.00	23.69	23.74	30.32
		Uncorrelated relaxed log normal	Constant	-23.25	-25.98	-23.69	0.00	0.06	6.64
			GMRF SkyRide	-23.30	-26.03	-23.74	-0.06	0.00	6.58
			Bayesian SkyGrid	-29.88	-32.62	-30.32	-6.64	-6.58	0.00
	Path sampling	Strict	Constant	0.00	5.84	6.66	30.15	32.28	37.83
			GMRF SkyRide	-5.84	0.00	0.82	24.31	26.44	31.99
			Bayesian SkyGrid	-6.66	-0.82	0.00	23.49	25.62	31.16
		Uncorrelated relaxed log normal	Constant	-30.15	-24.31	-23.49	0.00	2.13	7.68
			GMRF SkyRide	-32.28	-26.44	-25.62	-2.13	0.00	5.55
			Bayesian SkyGrid	-37.83	-31.99	-31.16	-7.68	-5.55	0.00